Technical note: How are NH$_3$ dry deposition estimates affected by combining the LOTOS-EUROS model with IASI-NH$_3$ satellite observations?

Shelley C. van der Graaf[1], Enrico Dammers[2], Martijn Schaap[3,4], Jan Willem Erisman[1,5]

[1]Cluster Earth and Climate, Department of Earth Sciences, Vrije Universiteit Amsterdam, Amsterdam, 1081 HV, The Netherlands

[2]Environment and Climate Change Canada, Toronto, Ontario, ON M3H 5T4, Canada.

[3]TNO, Climate Air and Sustainability, Utrecht, 3584 CB, The Netherlands

[4]Institute for Meteorology, Free University Berlin, Berlin, 12165, Germany

[5]Louis Bolk Institute, Driebergen, 3972, The Netherlands

Correspondence to: Shelley C. van der Graaf (s.c.vander.graaf@vu.nl)

Abstract. Atmospheric levels of reactive nitrogen have increased substantially during the last century resulting in increased nitrogen deposition to ecosystems, causing harmful effects such as soil acidification, reduction in plant biodiversity and eutrophication in lakes and the ocean. Recent developments in the use of atmospheric remote sensing enabled us to resolve concentration fields of NH$_3$ with larger spatial coverage. These observations may be used to improve the quantification of NH$_3$ deposition. In this paper, we use a relatively simple, data-driven method to derive dry deposition fluxes and surface concentrations of NH$_3$ for Europe and for the Netherlands. The aim of this paper is to determine the applicability and the limitations of this method for NH$_3$. Space-born observations of the Infrared Atmospheric Sounding Interferometer (IASI) and the LOTOS-EUROS atmospheric transport model are used. The original modelled dry NH$_3$ deposition flux from LOTOS-EUROS and the flux inferred from IASI are compared to indicate areas with large discrepancies between the two. In these areas potential model or emission improvements are needed. The largest differences in derived dry deposition fluxes occur in large parts of Central Europe, where the satellite-observed NH$_3$ concentrations are higher than the modelled ones, and in Switzerland, northern Italy (Po Valley) and southern Turkey, where the modelled NH$_3$ concentrations are higher than the satellite-observed ones. A sensitivity analysis of 8 model input parameters important for NH$_3$ dry deposition modelling showed that the IASI-derived dry NH$_3$ deposition fluxes may vary from ~20% up to ~50% throughout Europe. Variations in the NH$_3$ dry deposition velocity led to the largest deviations in the IASI-derived dry NH$_3$ deposition flux and should be focused on in the future. A comparison of NH$_3$ surface concentrations with in-situ measurements of several established networks (EMEP, MAN and LML) showed no significant, or consistent improvement in the IASI-derived NH$_3$ surface concentrations compared to the originally modelled NH$_3$ surface concentrations from LOTOS-EUROS. It is concluded that the IASI-derived NH$_3$ deposition fluxes do not show strong improvements

compared to modelled NH_3 deposition fluxes and there is a future need for better, more robust, methods to derive NH_3 dry deposition fluxes.

1. Introduction

Reactive nitrogen (N_r) emissions have substantially increased during the last century to around four times the pre-industrial levels (Erisman et al., 2008;Fowler et al., 2013). As a result, atmospheric deposition of reactive nitrogen to both terrestrial and aquatic ecosystems has also increased (Dentener et al., 2006b). Excessive nitrogen deposition to sensitive ecosystems can cause harming effects such as soil acidification, reduction in plant biodiversity and eutrophication in water bodies (Erisman et al., 2015). One molecule of reactive nitrogen may even contribute to a number of these environmental impacts through different pathways and chemical transportation in the biosphere, the so-called nitrogen cascade (Galloway et al., 2003). Ammonia (NH_3) is one form of reactive nitrogen and constitutes an important part of the total amount of N_r emissions. Up to 50% of global reactive nitrogen emissions consist of NH_3 (Reis et al., 2009) and therefore NH_3 contributes significantly to these adverse effects. Atmospheric ammonia is deposited to surfaces by two processes: dry and wet deposition.

Dry deposition may comprise a large part of the total deposition. Earlier modelling studies showed that dry deposition of NH_x even constitutes to over 60% of the total deposition (Dentener et al., 2006a). The modelled fraction of dry deposition, however, ranges hugely depending on the used model. Deposition models in general are known to involve large uncertainties regarding the chemistry behind NH_4 formation and the NH_3 dry deposition velocities (Dentener et al., 2006a). At the same time, large-scale assessment of NH_3 dry deposition is hindered by the extremely limited number of dry deposition observations and their sparse distribution in space and time. Measurements of NH_3 dry deposition fluxes largely remain experimental and are limited to a few research sites and measurement campaigns of short durations (e.g. (Zoll et al., 2016;Spindler et al., 2001)). These measurements typically are representative for a confined area and a specific ecosystem. Dry deposition has so far been estimated on a regional scale through mainly two methods: geostatistical approaches and atmospheric chemistry models. Geostatistical approaches include geospatial interpolation of, or generating statistical models based on existing in-situ observations (e.g. (Erisman and Draaijers, 1995)). Atmospheric chemistry models use known and modelled inputs (i.a. emissions) to derive dry deposition fluxes (e.g. (Dentener et al., 2006a;Wichink Kruit et al., 2012;Van der Swaluw et al., 2017). Both methods depend strongly on the quality and availability of reliable input information, which is often limited or even absent.

Recent development in the use of atmospheric remote sensing to measure NH_3 distributions with large spatial coverage and daily resolution (Van Damme et al., 2014a) allow us to examine their development in space and time in more detail. Information from satellites can be of help to strengthen our understanding of the complex chain of processes of atmospheric deposition, emissions, dispersion and chemistry, especially when complemented with information from atmospheric chemistry models. Atmospheric chemistry models may for example help to fill in missing information on NH_3 concentrations close to the Earth's surface, arising from low sensitivities of NH_3 measuring instruments, or may, for instance, supplement satellite data with information on diurnal cycles. Nowlan et

al. (2014) estimated surface concentrations and dry deposition of NO_2 and SO_2 by combining satellite observations of the Ozone Monitoring Instrument (OMI) and the GEOS-Chem model. The resulting estimates compared reasonably well with in-situ measurements, thus providing a relatively simple, data-driven method to estimate surface concentrations and dry deposition fluxes on a worldwide scale. More recently, Kharol et al. (2017) derived NH_3 dry deposition fluxes over North-America using a similar method with NH_3 observations of the Cross-track Infrared Sounder (CrIS) satellite and the GEM-MACH model. The aim of this paper is to search for the applicability and the limitations of this method for NH_3 over Europe using space-born observations of the Infrared Atmospheric Sounding Interferometer (IASI) and the LOTOS-EUROS atmospheric transport model. This paper shows the first use of the IASI-NH_3 product for the derivation of NH_3 dry deposition fluxes, together with validation of the derived NH_3 surface concentrations with in-situ measurements. The latter serve as a direct proxy for the validity of the derived NH_3 dry deposition fluxes. Also, this paper is the first to estimate the effect of modelling errors on the satellite-derived NH_3 dry deposition fluxes by performing a model sensitivity study.

We start this paper with a description of the used models and datasets and their associated uncertainties. This is followed by a description of the methodology that is used to determine the NH_3 surface concentrations and dry deposition fluxes. Here we also describe the design of the sensitivity study of the LOTOS-EUROS model. The resulting estimates of the NH_3 surface concentrations and dry deposition fluxes are given. The NH_3 surface concentrations are compared to in-situ measurements from the EMEP network in Europe. In a special case study for the Netherlands, they are compared to in-situ measurements from the LML and the MAN networks. Moreover, a sensitivity study of the LOTOS-EUROS model is evaluated to estimate the effect of model input uncertainties on the results that are obtained in the same section. The study is then concluded with a discussion.

2. Models and datasets
2.1 IASI-NH_3 product

The Infrared Atmospheric Sounding Interferometer (IASI) is a passive remote-sensing instrument that measures infrared radiation emitted by the Earth's surface and atmosphere within the spectral range of 645-2769 cm^{-1} (Clerbaux et al., 2009). The IASI-A instrument is on board of the MetOp-A satellite that was launched in 2006 and circles in a polar sun-synchronous orbit. In this study, we used NH_3 total column measurements from the morning overpass, as these are more sensitive to NH_3 then the nighttime observations (Van Damme et al., 2015). The morning overpass passes over Europe once a day in the morning around 9:30. The NH_3 product has an elliptical spatial footprint of approximately 12 by 12 kilometers and a detection limit of 2.5 ppbv (Van Damme et al., 2015). The retrieval uses a neural network to derive NH_3 columns based on the calculation of the HRI (Hyperspectral Range Index), e.g. the spectral index (Van Damme et al., 2017). The retrieval algorithm combines information on the temperature, humidity and pressure profiles to represent the atmospheric state closely (Whitburn et al., 2016). The retrieval uses a fixed profile in time, based on the profiles described by Van Damme et al. (2015). The IASI-NN retrievals have been validated in Dammers et al. (2016) and Dammers et al. (2017b). In these papers, they compared the IASI-NN and FTIR total columns and showed that the two compare reasonably well with a systematic underestimation by the IASI-NN product of around 30%. In this paper, the NH_3 total columns observed during the

warmer season (April to September) of 2013 and 2014 are used. The warm season was chosen because considerably fewer observations are available during the cold months. Moreover, the observations in the cold months generally have a higher relative uncertainty (Van Damme, 2014). A filter has been applied after (Van Damme et al., 2014b). This filter leaves out observations with a relative error of <100% unless the absolute error is smaller than 5x 10^{15}

5   molecules cm^{-2}. Figure 1 shows the mean IASI NH_3 total column concentration over Europe and the Netherlands.
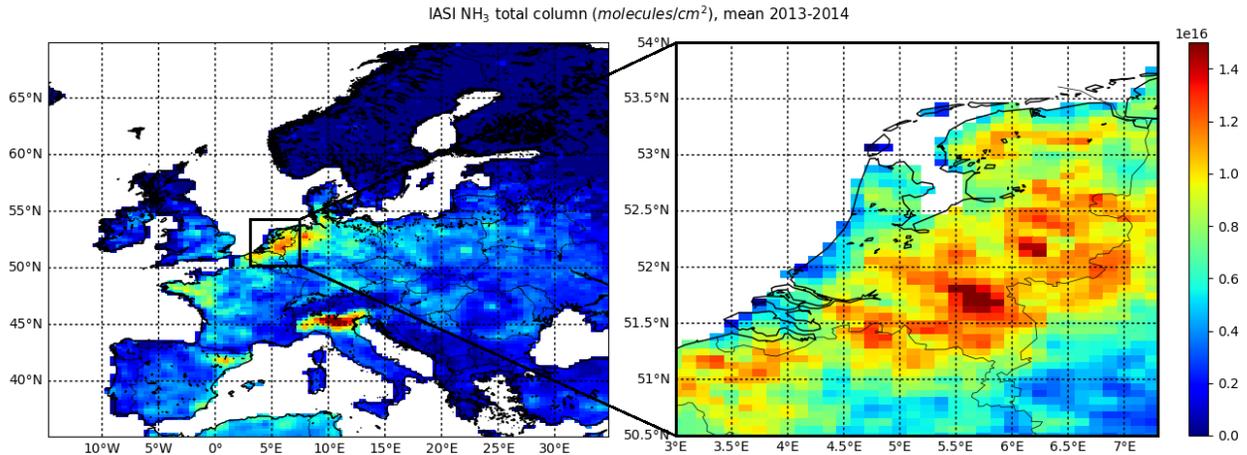

Figure 1: The annual mean NH₃ total column concentration in 2013- 2014 as observed by IASI-A in Europe (regridded to 0.50⁰ longitude by 0.25⁰ latitude) and the Netherlands (regridded to 0.125⁰ longitude by 0.0625⁰ latitude).

2.2 IASI NH₃ uncertainties

10   The retrieval algorithm (Whitburn et al., 2016) allows estimation of quantitative errors of each observation. The error estimate depends on a combination of the thermal contrast (the temperature difference between Earth's surface and atmosphere at 1.5km) and the HRI, i.e. the spectral footprint. The estimate also includes error terms for the uncertainty in the profile shape, and error terms arising from the used temperature and water vapor profiles. The uncertainty estimate for each retrieved NH_3 total column is an error propagation of the individual parameter

15   uncertainties. Whitburn et al. (2016) showed in an error characterization that individual retrieved NH_3 columns hold the smallest errors (~25%) in the situation of a high NH_3 concentration combined with a high thermal contrast. The error increases progressively when either of these lowers. In the case of a low NH_3 concentration and a low thermal contrast, the errors can be as high as ~270%. More information on how the IASI-NN retrieval works and how the relative errors are derived can be found in Whitburn et al. (2016). Figure 2 shows the relative uncertainty of the

20   IASI-A NH_3 total column concentrations in 2013-2014 over Europe and the Netherlands. The relative uncertainty ranges from ~90% in remote areas with little emissions to ~30% in high emissions areas.

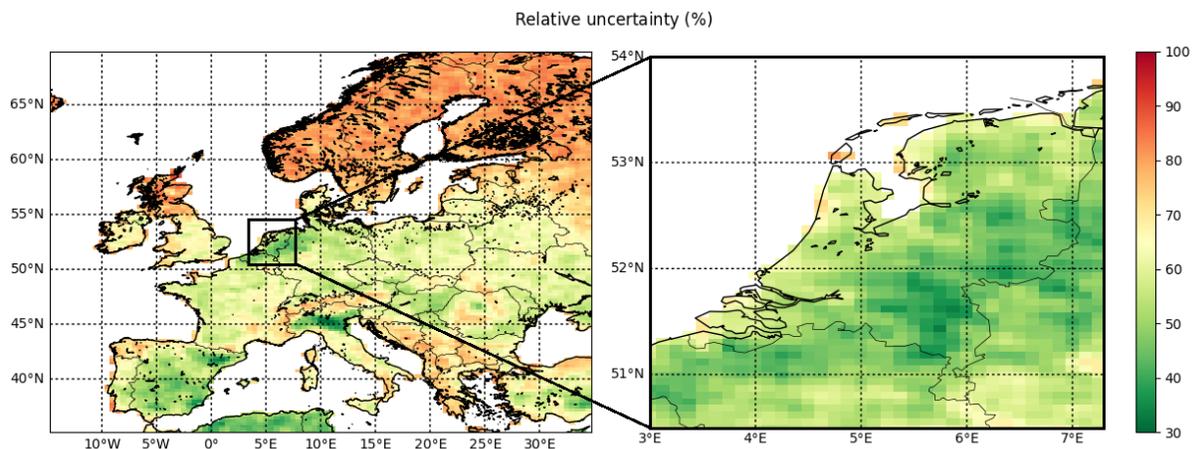**Figure 2: The relative error of the annual IASI-A retrieved NH$_3$ total column concentrations in Europe and the Netherlands in 2013-2014.**

2.3 NH$_3$ ground measurements

5   Ground measurements of NH$_3$ surface concentrations from three air quality networks were used to validate the LOTOS-EUROS and IASI-derived NH$_3$ surface concentrations on a monthly and a yearly basis. To do this, observations of ambient NH$_3$ concentrations of the EMEP (European Monitoring and Evaluation Program) network are used for Europe (EMEP, 2016). For the case study of the Netherlands observations from two established networks are used, the LML network (Landelijk Meetnet Luchtkwaliteit) (RIVM) and the MAN (Meetnet

10   Ammoniak in Natuurgebieden) (Lolkema et al., 2015).

NH$_3$ is challenging to measure reliably because of potential adsorption to parts of the measurement device, leading to slow response times (von Bobrutzki et al., 2010). The uncertainties of the measurements may differ significantly per instruments design. Table 1 gives an overview of the instruments used by each of these networks and their uncertainties.

15   #### 2.3.1   EMEP network

The main measurement network for reactive nitrogen concentrations on European-scale is the EMEP (European Monitoring and Evaluation Program) network (Tørseth et al., 2012). NH$_3$ measurements from 35 stations were available to validate the results of 2013 and 46 stations for the results of 2014. Different types of measurement devices are used to measure NH$_3$ within the EMEP network. The majority of the EMEP sites use filter-packs, of

20   which the results are relatively uncertain. In a field intercomparison of different NH$_3$ measurement techniques, von Bobrutzki et al. (2010) found that different instruments have an overall bias varying from -31.1% to +10.9% for the entire data range (~two weeks), demonstrating that there is a need for a standardized approach. For smaller concentrations (<10 ppbv) the bias is even larger, from -22.0% to +54.5%.

2.3.2   LML network

25   The LML monitors hourly NH$_3$ concentrations in the Netherlands since 1993 (van Zanten et al., 2017). Since 2014

5

only 6 stations are left in operation, before that there were 8 stations. The locations of the monitoring stations were carefully selected to cover regions with high, moderate and low emission densities equally. The measurements are performed with AMOR instruments, which are continuous flow denuders. Airflow passes through a wetted rotating denuder tube in the AMOR instrument and the NH_3 absorbs into this fluid. The electric conductivity is then determined and used as a measure for the NH_3 concentration (van Zanten et al., 2017). The measurements have a reported uncertainty of at least 9% for hourly concentrations and at least 7% for yearly averages (van Zanten et al., 2017;Blank, 2001).

2.3.3   MAN network

The MAN network provides monthly mean ambient NH_3 concentrations in nature areas in the Netherlands since 2005. The network has 236 sampling points since 2014, spread over 60 different nature areas. The measurements are performed with low-cost passive samplers from Gradko. The measurements are calibrated against the measurements of the LML (Lolkema et al., 2015). The bottom of the passive sampler is an open cap with a porous filter through which NH_3 in the air can enter. In the top end of the tube, the NH_3 is adsorbed by an acid to form NH_4^+. The NH_4^+ concentrations in the samplers are analyzed in a laboratory every month to compute the monthly mean NH_3 concentrations. The uncertainty of the MAN measurements depends on the NH_3 concentration and varies between 20% for high concentrations (10-20 μgm^{-3}) and 41% for low concentrations (1 μgm^{-3}) (Lolkema et al., 2015).

Network	Instrument(s)	Uncertainty
EMEP	Filter-packs, denuders	~20 – 25 % (yearly means)
MAN	Passive samplers	20 – 41% (monthly means) (Lolkema et al., 2015)
LML	Continuous-flow denuders (AMORs)	> 9% (hourly measurement), > 7% (observed annual means) (Blank, 2001)

Table 1: Type of instruments used to measure ambient NH_3 concentrations and associated uncertainty estimates.

2.4   The LOTOS-EUROS model

2.4.1   Model description

LOTOS-EUROS is an Eulerian chemistry transport model (CTM) (Manders et al., 2017) that simulates air pollution in the lower troposphere. A horizontal resolution of 0.50º longitude by 0.25º latitude, corresponding to approximately 28 by 28 km^2 is used to perform simulations for Europe (35ºN - 70ºN, 15ºW -35ºE). Secondly, for the case study of the Netherlands the horizontal resolution is set to 0.125º longitude by 0.0625º latitude, approximately 7 by 7 km (50.5 ºN - 54ºN, 3ºE -7.5ºE). The vertical resolution of the model is a four-layer vertical grid that extends up to 3.5 km above sea level. The bottom layer is the surface layer and has a fixed height of 25 meters. On top of this layer, there is a mixing layer, followed by two equally thick dynamic reservoir layers with time-varying thicknesses. The model follows the mixed layer approach. LOTOS-EUROS performs hourly calculations using meteorology provided by ECMWF (ECMWF, 2016). Gas-phase chemistry is described using the TNO CBM-IV scheme (Schaap et al., 2009), which is an updated version of the original scheme by (Whitten et al., 1980). Anthropogenic emissions used in LOTOS-EUROS are taken from the TNO-MACC-III emission database (Kuenen

et al., 2014). LOTOS-EUROS uses a set of temporal factors (monthly, daily and hourly) to break down annual total emissions into hourly emissions. The time profile of a particular pollutant is an aggregation of the time-dependent emission strengths from different SNAP (Selected Nomenclature for Sources of Air Pollution) sources. The monthly NH_3 emissions peak in March and then decrease, followed by another smaller peak in September. The daily NH_3 emission strengths are re-distributed more or less evenly over the week. The hourly NH_3 emission peak is reached at 13.00 h (Denier van der Gon et al., 2011).

2.4.2 Dry deposition parameterization

The dry deposition fluxes in LOTOS-EUROS are calculated with the DEPAC3.11 (Deposition of Acidifying Compounds) module, following the resistance approach (van Zanten et al., 2010). In this approach, the deposition velocity is the reciprocal sum of the aerodynamic resistance, the quasi-laminar layer resistance and the surface resistance. A canopy compensation point for simulation of the bi-directional flux of NH_3 is included in the implementation of the DEPAC3.11 module, following the approach presented in Wichink Kruit et al. (2012). The compensation point is computed dynamically using modelling results from the last month. The model uses the CORINE/Smiatek land use map converted to the DEPAC land use classes to determine the exchange velocities for different land use classes. More information on the LOTOS-EUROS model can be found in Manders et al. (2017).

2.4.3 Model performance

The LOTOS-EUROS model has participated in multiple model intercomparison studies (e.g. (Colette et al., 2017;Wichink Kruit, 2013;Bessagnet et al., 2016;Vivanco et al., 2018)), showing an overall good model performance. LOTOS-EUROS also showed a good correspondence with yearly NH_3 concentrations with a slight underestimation in agricultural areas and overestimation in nature areas in the Netherlands (Wichink Kruit, 2013). The inferential method that we use here heavily relies on results from LOTOS-EUROS. The model therefore has to closely represent reality, if we wish to obtain reasonable results. As in any model, there are, however, uncertainties associated with every part of the total chain of modelled processes. The uncertainties related to emissions and to dry and wet deposition are expected to impact the results the most and are discussed below.

2.4.4 Uncertainties related to emission input

Emissions are the most important input for any CTM and are, at the same time, a source of substantial uncertainties (Reis et al., 2009;Behera et al., 2013). NH_3 emissions are relatively uncertain due to the diverse nature of agricultural sources leading to large spatial and temporal variations in emissions. The uncertainty of the European reported annual totals is estimated to be around ±30% (EMEP, 2016). The uncertainty is larger for countries that have limited research on their emission inventory and carry out a few emission measurement activities.

The presence of other gaseous components such as SO_2 and NO_x may have a high impact on the modelled NH_3 concentrations, as NH_3 in the atmosphere reacts readily with sulfuric acid (H_2SO_4) and nitric acid (HNO_3) to form particulate ammonium (e.g. ($NH_4)_2SO_4$ or NH_4NO_3). It is therefore also important to consider the errors in the SO_2 and NO_x emissions. The SO_2 emissions are relatively well known per source category and thus hold a relatively low uncertainty of about ±10% on reported annual totals. The uncertainty in the NO_x emissions is higher, of around

±20% on reported annual totals. However, due to interpolation to account for missing data for some countries, the final uncertainty of the annual totals of both SO_2 and NO_x is estimated to be higher (Kuenen et al., 2014).

Needless to say, one single emission at a certain time may have a much higher error due to the large uncertainty related to redistribution and the timing of emissions (Hendriks et al., 2016;Skjøth et al., 2011). More information on the quality data ratings of NH_3, SO_2 and NO_x per source category and per country can be found in the report of the European Environment Agency (EEA, 2016).

2.4.5 Uncertainties regarding dry and wet deposition

The second source of uncertainties originates from the model parameterization of both dry and wet deposition. Several multi-model studies (e.g. (Dentener et al., 2006a;Colette et al., 2017;Wichink Kruit, 2013;Flechard et al., 2011;Vivanco et al., 2018) have shown that there is quite a large discrepancy in the implementation of dry and wet deposition in different CTMs. A fundamental input for estimating dry deposition fluxes in CTMs is the uncertainty in the deposition velocity. Schrader and Brummer (2014) compiled a database of the NH_3 deposition velocities per land use category that have been used in several deposition models from 2004 to 2013. The results showed quite a large variation in the V_d values for different land use classes. Some classes (e.g. water, urban) showed only a small variation in V_d of an interquartile range of ~5 to 10% for 50% of the data. Other classes (e.g. coniferous, agriculture) showed a much larger interquartile range in V_d of ~30 to 40%. Flechard et al. (2011) compared four existing dry deposition routines across 55 N_r monitoring sites and found that the differences between models reach a factor 2-3 and are often larger than differences between monitoring sites. Erisman (1993) estimated the dry and wet deposition fluxes of acidifying substances in the Netherland from measured and modelled concentrations. The estimated uncertainty in the average NH_3 fluxes in this paper was estimated to be 30%, with a systematic error of 30% in the used V_d for NH_3. Dentener et al. (2006a) calculated the deposition of N_r with 23 atmospheric chemistry transport models in a multi-model evaluation. Although there were quite large differences between the different models, the paper showed that 71.7% of the model-calculated mean wet deposition rates in Europe agreed to within ±50% with NH_4^+ wet deposition measurements from the EMEP network.

3 Methodology

The NH_3 surface concentrations and dry deposition fluxes are estimated by combining the observations of the IASI-A satellite instrument and the modelling results from LOTOS-EUROS. The method is an adapted version of the approach for NO_2 and SO_2 presented by Nowlan et al. (2014). The IASI-A instrument only observes the NH_3 total column at overpass time. We use the modelling results of LOTOS-EUROS to account for the diurnal variation in the atmospheric concentrations of NH_3. The vertical NH_3 profiles in LOTOS-EUROS are also used to deduce the ground-level NH_3 concentrations from IASI. The computation of the IASI-derived NH_3 surface concentrations and dry deposition fluxes is described in detail in the following sections.

3.1 Surface concentration computation

The NH$_3$ total column observations from IASI are first regridded onto the LOTOS-EUROS model grid. The monthly mean NH$_3$ total column concentrations are then calculated for each pixel. We use the vertical profile of NH$_3$ per grid cell in LOTOS-EUROS to relate the IASI NH$_3$ total column to NH$_3$ surface concentrations. The IASI-derived NH$_3$ surface concentrations C^{IASI} are computed following Eq. (1):

$$5 \quad C^{IASI} = \frac{\Omega^{IASI}}{\Omega^{LE}_{overpass}} \cdot C^{LE} \quad\quad\quad (1)$$

Here Ω^{IASI} represents the monthly mean NH$_3$ total column concentration from IASI (molecules cm^{-2}), $\Omega^{LE}_{overpass}$ represents the modelled NH$_3$ total column at overpass time in LOTOS-EUROS (molecules cm^{-2}) and C^{LE} is the modelled mean surface concentration (μg m^{-3}), the concentration in the down-most layer in LOTOS-EUROS.

3.2 Dry deposition flux computation

10 The hourly NH$_3$ dry deposition fluxes are modelled in LOTOS-EUROS. The modelled NH$_3$ dry deposition fluxes are then adjusted based on actual observations from IASI. The modelled and the IASI-derived NH$_3$ concentrations share the same vertical profile. The ratio of the observed and the modelled total column concentrations, rather than the surface concentrations, is therefore directly used to alter the modelled NH$_3$ dry deposition flux. The NH$_3$ dry deposition flux (kg N ha^{-1}yr^{-1}) inferred from IASI, F^{IASI}, is computed following Eq. (2):

$$15 \quad F^{IASI} = \frac{\Omega^{IASI}}{\Omega^{LE}_{overpass}} \cdot F^{LE}_{daily} \quad\quad\quad (2)$$

Here Ω^{IASI} denotes the NH$_3$ total column concentration from IASI, $\Omega^{LE}_{overpass}$ the modelled NH$_3$ total column at overpass time in LOTOS-EUROS (molecules cm^{-2}) and F^{LE}_{daily} the total daily NH$_3$ dry deposition flux in LOTOS-EUROS (kg N ha^{-1}yr^{-1}). F^{LE}_{daily} is the sum of the hourly NH$_3$ dry deposition fluxes, as shown in Eq. (3):

$$F^{LE}_{daily} = \sum_{h=1}^{24} F^{LE}_h = \sum_{h=1}^{24} V_d \left(C^{LE}_h - \chi^{LE}_{tot,h}\right) \quad\quad\quad (3)$$

20 The hourly NH$_3$ dry deposition flux is the product of the dry deposition velocity V_d and the difference between the hourly NH$_3$ surface concentration, C^{LE}_h, and the total compensation point of NH$_3$, $\chi^{LE}_{tot,h}$. To account for the high variability of atmospheric NH$_3$ and the limiting amount of available IASI observations, monthly means of these values are used rather than daily values.

3.3 Sensitivity analysis

25 The main sources of model uncertainties that are relevant for deposition modelling arise from uncertainties in the emission input and the deposition parameterizations (see Section 2.3).

A total of 4 input fields were varied in LOTOS-EUROS: the MACC-III NH$_3$ emissions, the MACC-III NO$_x$ and SO$_2$ emissions, the dry deposition velocity, V_d, of NH$_3$ and the wet deposition of NH$_3$. The wet deposition is varied by adjustment of the gas scavenging constant, G$_{scav}$, for NH$_3$. The wet scavenging constant G$_{scav}$ linearly influences the

amount of NH_3 wet deposition. This results in changes in the wet NH_3 deposition flux of +30% and -30%, too. The objective of these 8 sensitivity runs is to assess the uncertainty ranges on the estimated dry NH_3 deposition fluxes resulting from modelling errors. Table 2 gives an overview of the parameters that are varied. We chose to apply a constant perturbation of +30% and -30% to one field at the time to see their individual effect and to improve the comparability of the results, too. Moreover, perturbations of ±30% are reasonable ranges since they correspond to the estimated uncertainties in the MACC-III emission fields annual totals and the uncertainties in the wet and dry deposition fluxes of NH_3.

Perturbed parameter	Perturbations
MACC-III NH_3 emissions	+30%, -30%
MACC-III NO_x and SO_2 emissions	+30%, -30%
NH_3 dry deposition velocity, V_d^{NH3}	+30%, -30%
NH_3 gas scavenging coefficient, G_{scav}^{NH3}	+30%, -30%

Table 2: Perturbations on input fields that have been used for the sensitivity analysis of the method.

4   Results

4.1   NH$_3$ surface concentrations

4.1.1   Europe

Figure 3 shows the warm season (April-September) mean NH_3 surface concentrations in 2013 and 2014. The left figures show the modelled concentrations from LOTOS-EUROS (which we will refer to as the 'modelled concentrations') and concentrations that are derived from IASI in combination with LOTOS-EUROS (which we will refer to as 'IASI-derived concentrations'). The dots represent the corresponding measurements from the EMEP stations. The right figures show the absolute differences between the EMEP measurements and the modelled and IASI-derived concentrations. In general, the pattern of the EMEP measurements and the modelled and IASI-derived concentrations matches quite well. The majority of the EMEP measurements agrees with the modelled and IASI-derived concentrations to -0.75 to +0.75 μgm^{-3}. The sum of the absolute differences between the warm season mean NH_3 surface concentrations in a cubic meter from EMEP and LOTOS-EUROS was 23.0 µg in 2013 and 32.5 µg in 2014. The sum of the absolute differences between the warm season mean NH_3 surface concentrations from EMEP and IASI was slightly lower, 22.6 µg in 2013 and 28.0 µg in 2014.
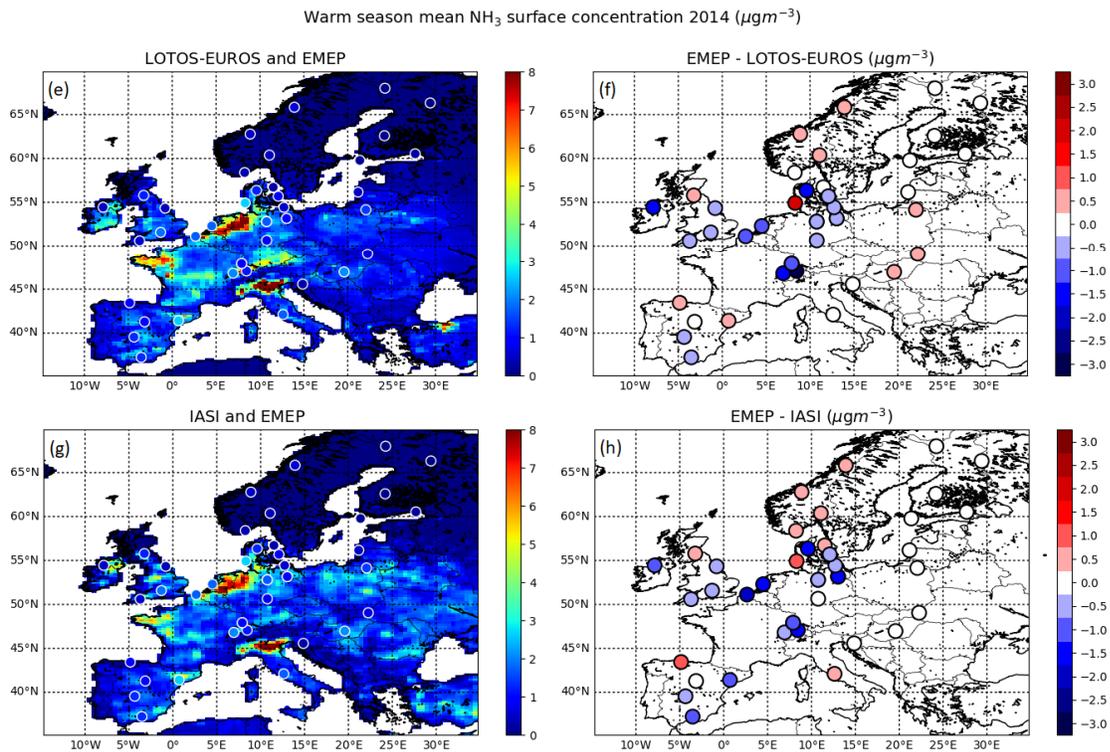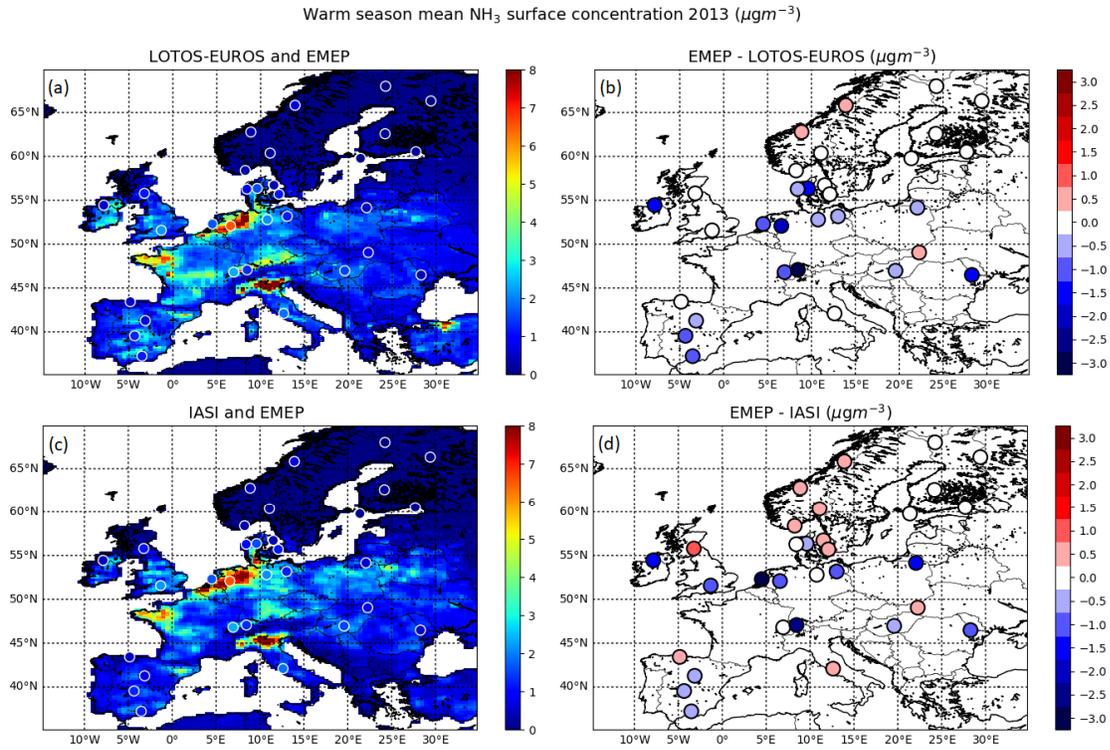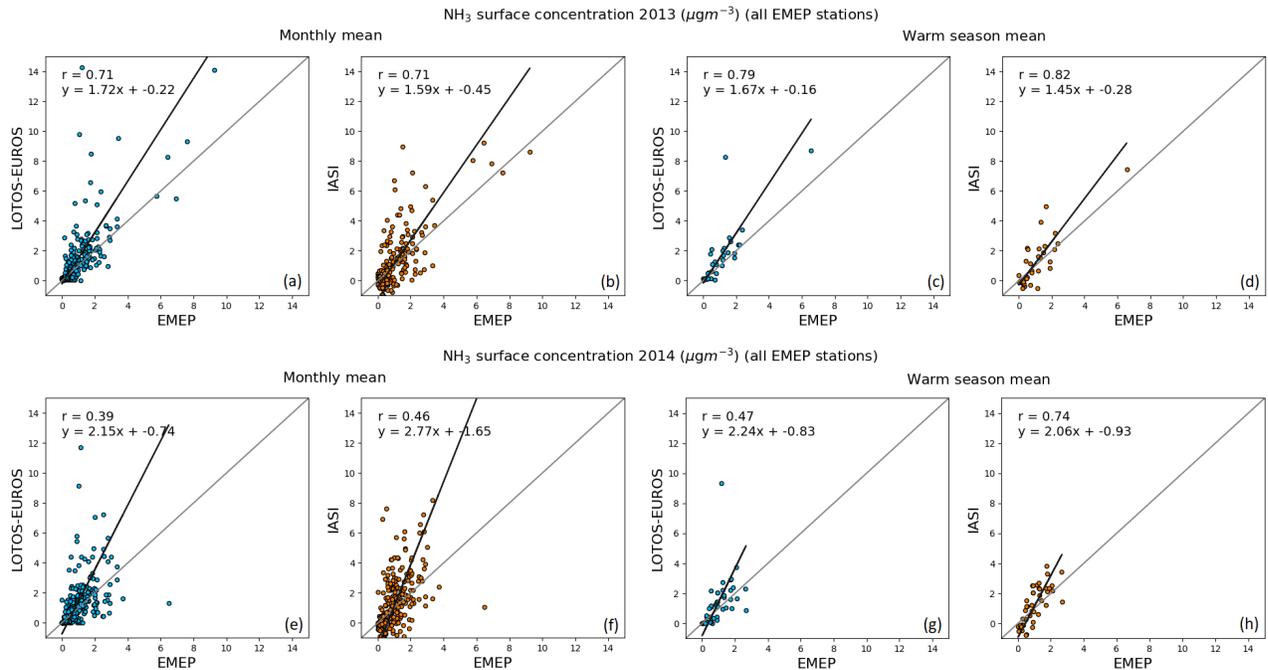
Figure 3: Comparison of the warm season (April-September) mean NH₃ surface concentrations (μgm⁻³) from LOTOS-EUROS and derived from IASI and the warm season mean NH₃ surface concentrations measured by the EMEP stations in 2013 (a, b, c, d) and 2014 (e, f, g, h). The absolute differences between the two are shown in the right figures.

Figure 4 shows scatterplots of the monthly mean (left) and the warm season mean (right) NH_3 surface concentrations. The x-axis represents concentrations measured by the EMEP stations. The y-axis represents either the modelled concentrations (blue) or the IASI-derived concentrations (orange). The monthly mean modelled concentrations and the EMEP measurements show a reasonably strong linear relationship in 2013 (r =0.71). The correlation between the two was weaker (r = 0.39) in 2014. The correlation between the IASI-derived concentrations and the EMEP measurements was similar in 2013 (r = 0.71), and was higher in 2014 (r = 0.46). The warm season mean IASI-derived concentrations and the EMEP measurements have a slightly stronger correlation coefficient and an improved slope compared to the modelled concentrations.

Figure 4: Comparison of the monthly mean (a, b, e, f) and warm season (April-September) mean (c, d, g, h) NH_3 surface concentrations measured by the EMEP stations and the corresponding NH_3 surface concentrations from LOTOS-EUROS (blue dots) and inferred from IASI (orange dots) in 2013 (top) and 2014 (bottom).
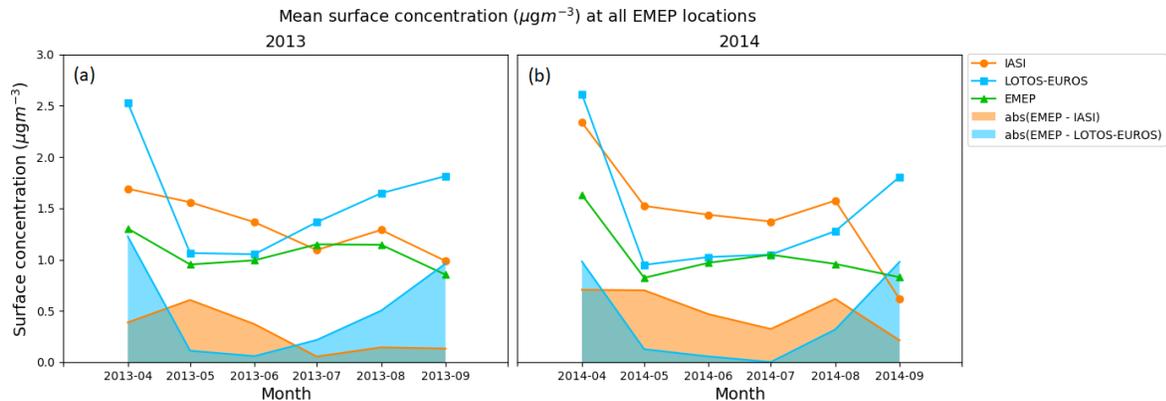
Figure 5: Mean of the NH_3 surface concentrations at all EMEP locations per month (green line), and the coinciding NH_3 surface concentrations from LOTOS-EUROS (blue line) and derived from IASI (orange line) in 2013 (a) and 2014 (b).

The absolute differences between EMEP and LOTOS-EUROS are shown in blue and the absolute differences between EMEP and IASI are shown in orange.

Figure 5 shows the mean NH_3 surface concentration of all EMEP stations per month, and the corresponding modelled and IASI-derived concentrations at the same locations. The absolute differences per month are plotted in the same figure in blue (LOTOS-EUROS vs EMEP) and orange (IASI-derived vs EMEP). All concentration time profiles show a peak value in April, resulting from spring fertilization. The LOTOS-EUROS time profile at the EMEP locations decreases from April to May and starts to increase towards the end of the year. The time profile of the EMEP stations follows the same pattern from April to June, but decreases towards the end of the year. The IASI-derived time profile shows a decreasing pattern, except in August, where there is a small peak. The IASI-derived time profile shows a relatively better comparison with the EMEP measurements in April and July to September in 2013 and in April and September in 2014. The sum of the absolute differences of the mean NH_3 surface concentrations in a cubic meter at all EMEP locations between LOTOS-EUROS and EMEP amounts to 3.1 µg in 2013 and 2.5 µg in 2014. The sum of the absolute differences between IASI and EMEP was somewhat smaller in 2013, amounting to 1.7 µg, and somewhat higher in 2014, amounting to 3.0 µg.

In summary, the majority of the IASI-derived concentrations showed a slightly stronger correlation with the EMEP measurements than modelled concentrations on a monthly basis. The correlation became more pronounced on a seasonal basis (mean of April-September).

4.1.2   The Netherlands

4.1.2.1   Comparison with LML measurements

Figure 6 shows the warm season (April-September) mean NH_3 surface concentrations (μgm^{-3}) in the Netherlands in 2013 and 2014. The corresponding LML measurements are plotted on top of the modelled and IASI-derived concentrations. LOTOS-EUROS seems to capture the general pattern of the LML measurements fairly well in both 2013 and 2014. The sum of the absolute differences between the warm season mean NH_3 surface concentrations in a cubic meter from LML and LOTOS-EUROS was 47.3 µg in 2013 and 44.8 µg in 2014. The sum of the absolute differences between the warm season mean NH_3 surface concentrations from LML and IASI was slightly lower in 2013, namely 44.9 µg, and somewhat higher in 2014, namely 48.5 µg.

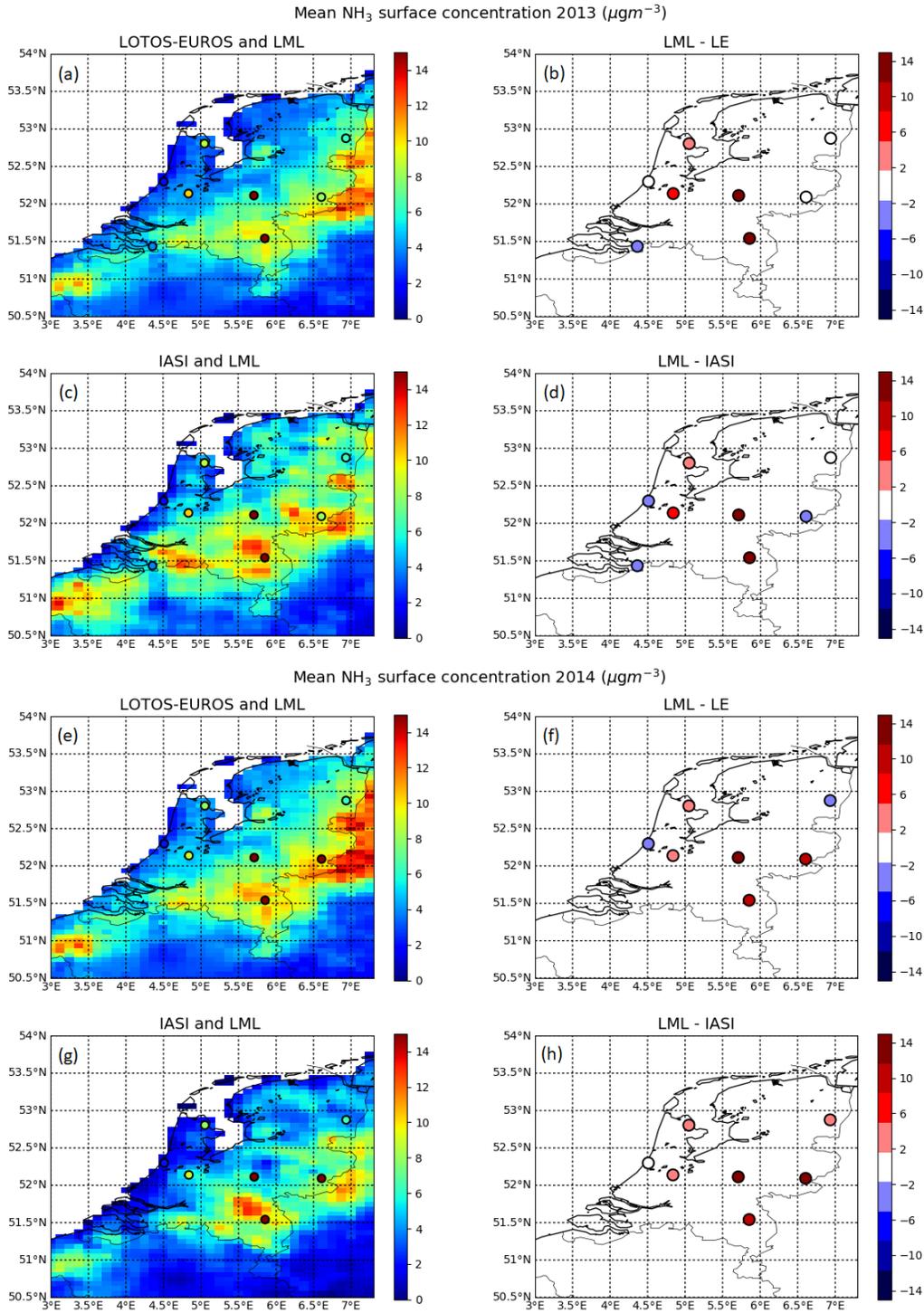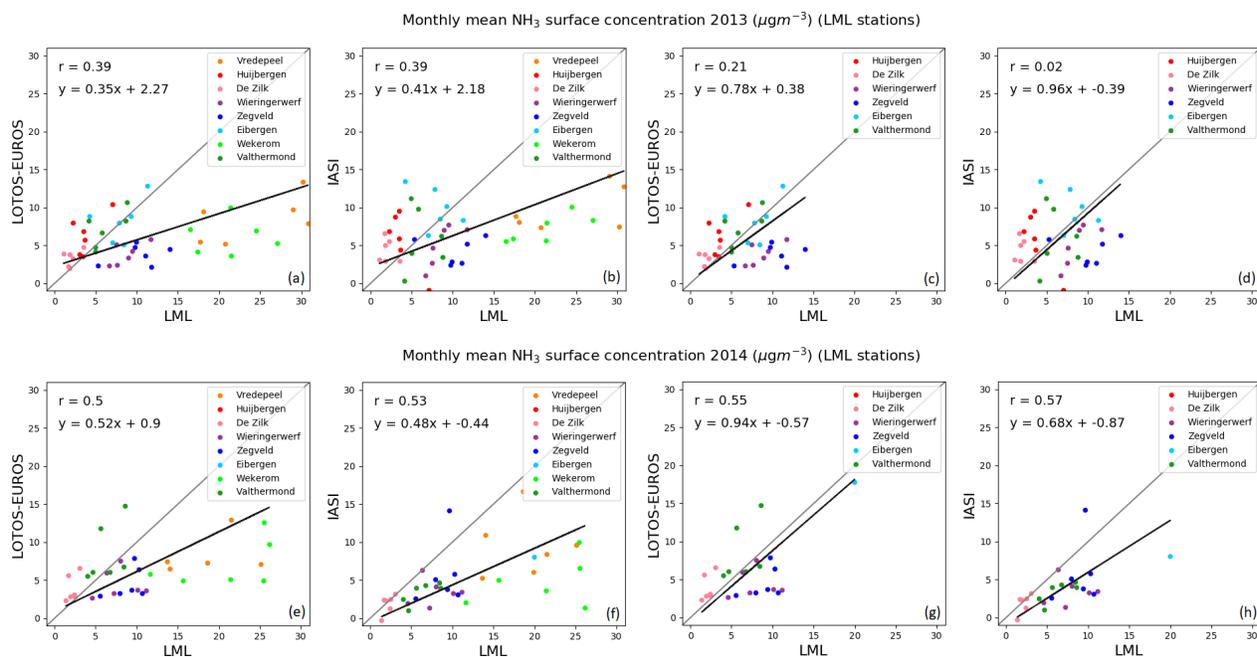Mean NH$_3$ surface concentration 2013 ($\mu g m^{-3}$)

Figure 6: Comparison of the warm season (April-September) mean NH$_3$ surface concentration in 2013 (a, b, c, d) and in 2014 (e, f, g, h) from LOTOS-EUROS and derived using IASI. The corresponding warm season mean NH$_3$ surface concentrations measured by the LML stations are plotted on top of the left figures. The right figures depict the differences between the two.

5

14

Figure 7 shows scatterplots of the monthly mean NH_3 surface concentrations (μgm^{-3}). The x-axis depicts the LML measured concentrations. The y-axis depicts the corresponding modelled and IASI-derived concentrations. The modelled concentrations and the LML measurements show a moderate linear relationship (r =0.39 in 2013, r = 0.50 in 2014). The high NH_3 concentration stations Vredepeel and Wekerom are underestimated by LOTOS-EUROS. The other stations are closer to the one-on-one line and appear to match quite well. The correlation coefficient of the IASI-derived concentrations and the LML measurements is r =0.39 in 2013 and r = 0.53 in 2014. The IASI-derived concentrations also underestimate the high concentration LML stations (Vredepeel and Wekerom) in both years. The majority of the low concentration LML stations are overestimated by the IASI-derived concentrations in 2013, and underestimated by the IASI-derived concentrations in 2014. In general, both high and low LML measurements were reproduced inadequately by the IASI-derived concentrations. The elimination of the high concentration stations Vredepeel and Wekerom does not lead to a better comparison of the LML measurements to the IASI-derived concentrations.

Figure 7: Comparison of the monthly mean NH_3 surface concentrations measured by the LML stations and the corresponding LOTOS-EUROS and IASI-derived NH_3 surface concentrations during the warm season (April-September) of 2013 (top) and 2014 (bottom). The high concentration stations Vredepeel and Wekerom are eliminated from the right figures (c, d, g, h).

Table 3 gives a month by month comparison of the correlation coefficient, the slope and the intercept of the monthly mean NH_3 surface concentrations of all LML stations versus the corresponding modelled and IASI-derived concentrations. In 5 out of 12 months the IASI-derived concentrations and the LML measurements have a better correlation coefficient and the slope compared to the modelled concentrations and the LML measurements. The modelled concentrations are consistently lower than the LML measurements.

In short, the IASI-derived concentrations do not show a better comparability with the LML measurements compared to the modelled concentrations.

	Month	LOTOS-EUROS				IASI-derived			
		R	slope	intercept	RMSD	r	slope	intercept	RMSD
LML	04-2013	0.57	0.39 ↑	4.12	7.78 ↑	0.57	0.36	0.01 ↑	10.80
	05-2013	0.49 ↑	0.19 ↑	2.16 ↑	7.53	-0.21	-0.30	9.61	7.20 ↑
	06-2013	0.38	0.19	1.73 ↑	8.58	0.44 ↑	0.45 ↑	1.74	6.80 ↑
	07-2013	0.36	0.18	3.31 ↑	11.67	0.46 ↑	0.34 ↑	3.74	10.00 ↑
	08-2013	0.49	0.23	3.82	10.10	0.86 ↑	0.35 ↑	3.63 ↑	7.93 ↑
	09-2013	0.27 ↑	0.33	4.28	5.79 ↑	0.04	0.65 ↑	0.38 ↑	7.31
	04-2014	0.69 ↑	0.56 ↑	4.36	5.81 ↑	0.21	0.46	0.44 ↑	10.32
	05-2014	0.39	0.29	1.90 ↑	6.35	0.76 ↑	0.72 ↑	-2.79	6.15 ↑
	06-2014	0.63	0.20	2.31	9.65	0.85 ↑	0.66 ↑	-0.99 ↑	6.60 ↑
	07-2014	0.70 ↑	0.19	2.27	10.53	0.68	0.29 ↑	1.22 ↑	10.19 ↑
	08-2014	0.68 ↑	0.47 ↑	0.75	4.97 ↑	0.46	0.31	0.69 ↑	6.50
	09-2014	0.55 ↑	0.33 ↑	4.84	8.20 ↑	0.04	0.27	1.49 ↑	11.59

Table 3: Month by month comparison of the correlation coefficient (r), slope and intercept of the monthly mean NH_3 surface concentrations of the LML stations (x-axis) and the coinciding monthly mean LOTOS-EUROS and IASI-derived NH_3 surface concentrations (y-axis). The green arrows denote which of the two (LOTOS-EUROS or IASI) gives the most desirable value. The green arrows are attributed to either LOTOS-EUROS or IASI based on the following criteria: highest r, slope closest to 1, intercept closest to 0 and smallest RMSD.

4.1.2.2 Comparison with MAN measurements

Figure 8 shows the warm season mean NH_3 surface concentrations in the Netherlands in 2013 and 2014. The dots represent the corresponding MAN measurements. The patterns of the MAN measurements are captured quite well by the modelled concentrations, with low NH_3 surface concentrations near the coast, and increasing values towards the east of the Netherlands. The sum of the absolute differences between the warm season mean NH_3 surface concentrations in a cubic meter from MAN and LOTOS-EUROS was 444.7 µg in 2013 and 494.3 µg in 2014. The sum of the absolute differences between the warm season mean NH_3 surface concentrations from MAN and IASI was slightly higher in both years, amounting to 512.1 µg in 2013 and 513.6 µg in 2014.
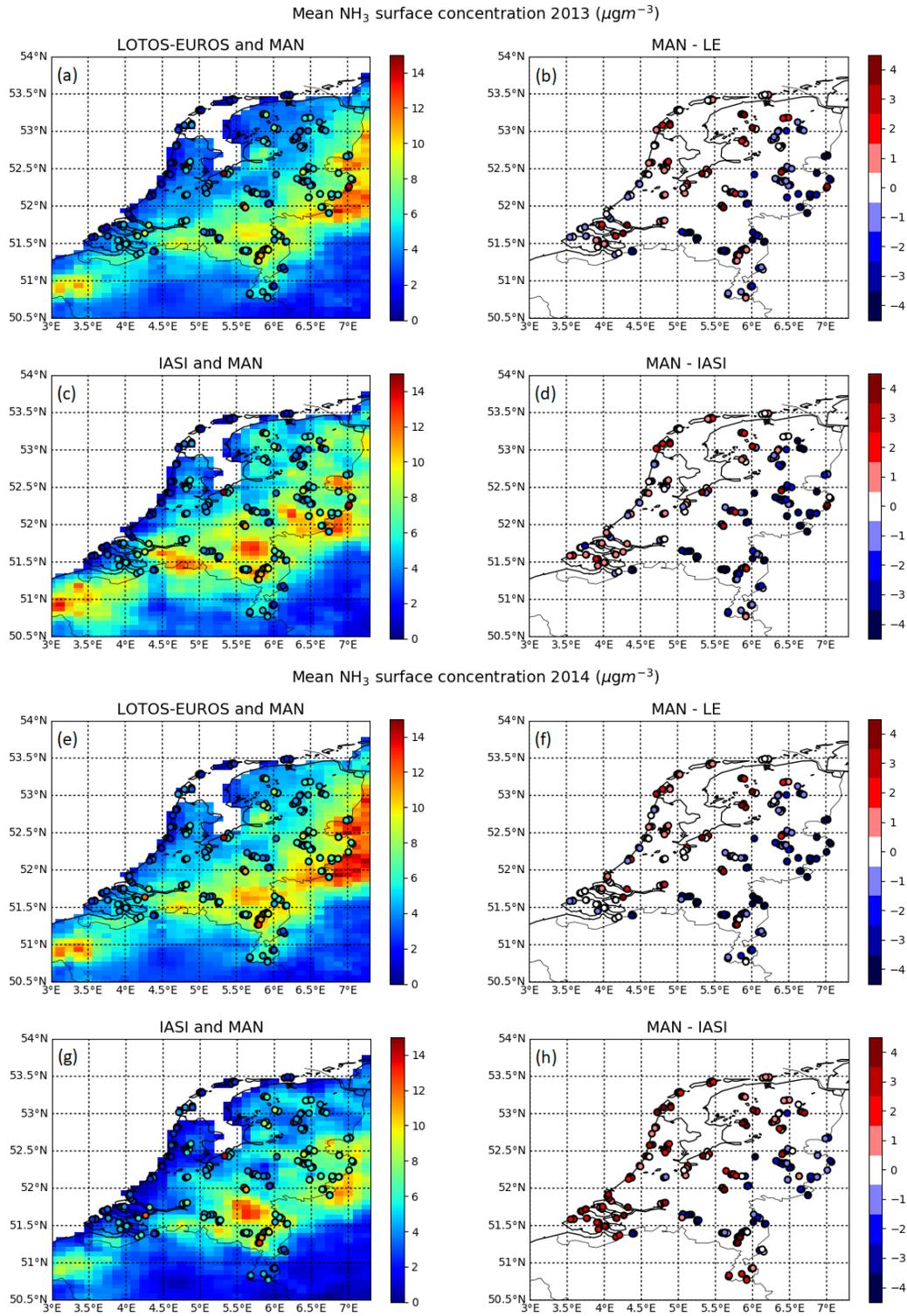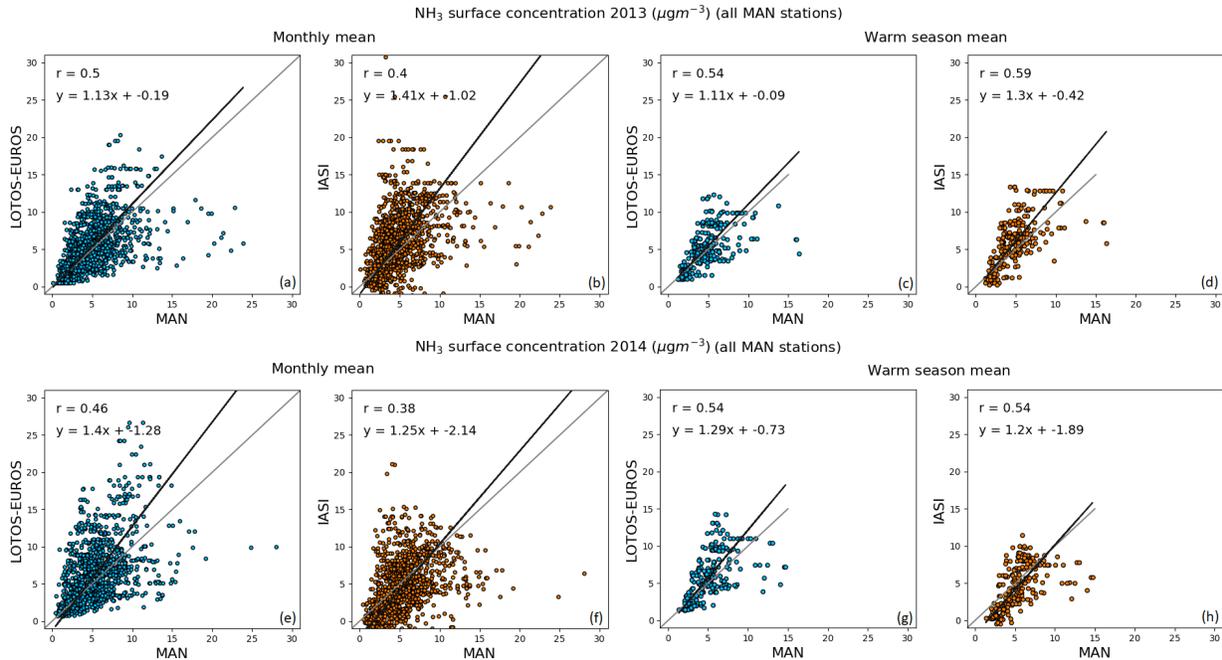
Figure 8: Comparison of the warm season (April-September) mean NH₃ surface concentration in 2013 (a, b, c, d) and in 2014 (e, f, g, h) from LOTOS-EUROS and derived using IASI. The corresponding warm season mean NH₃ surface concentrations measured by the MAN stations are plotted on top of the left figures. The right figures depict the differences between the two.

Figure 9 shows scatterplots of the monthly mean (left) and warm season mean (right) NH_3 surface concentrations. The x-axis depicts the MAN measurements. The y-axis depicts the corresponding modelled or IASI-derived concentrations. The modelled concentrations and the MAN measurements show a moderate positive linear relationship (r =0.5 in 2013, r = 0.46 in 2014). The correlation of the IASI-derived concentrations and the MAN measurements is somewhat weaker in both years (r = 0.40 in 2013, r = 0.38 in 2014). The IASI-derived concentrations and the MAN measurements show a similar to slightly stronger correlation (r = 0.59 in 2013, r = 0.54 in 2014) compared to the modelled concentrations and the MAN measurements for the warm season (r = 0.54 in 2013, r = 0.54 in 2014).

Figure 9: Comparison of the monthly mean (left) and warm season (April-September) mean (right) NH_3 surface concentrations measured by the MAN stations and the corresponding NH_3 surface concentrations from LOTOS-EUROS (blue dots) and inferred from IASI (orange dots) in 2013 (top) and 2014 (bottom).
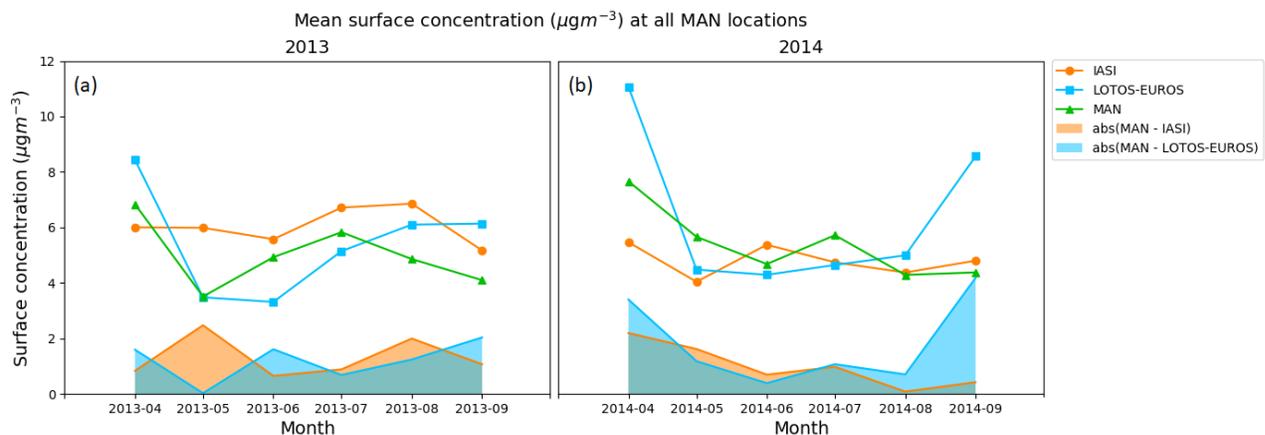
Figure 10: Mean of the NH_3 surface concentrations at all MAN locations per month (green line), and the coinciding NH_3 surface concentrations from LOTOS-EUROS (blue line) and IASI (orange line) in 2013 (a) and 2014 (b). The absolute

18

differences between MAN and LOTOS-EUROS are shown in blue and the absolute differences between MAN and IASI are shown in orange.

Figure 10 shows the mean NH_3 surface concentration of all MAN stations per month, and the corresponding modelled and IASI-derived concentrations at the same locations. The absolute differences per month are plotted in blue (LOTOS-EUROS vs MAN) and orange (IASI-derived vs MAN). The mean of all MAN stations peaks in April in both years. In 2013, the mean of all MAN stations increases from May on, peaks in July and then decreases towards the ending of the year. In 2014, there is an additional peak in July, followed by another decrease.

The sum of the absolute differences of the mean NH_3 surface concentrations in a cubic meter at all MAN locations between LOTOS-EUROS and MAN amounts to 7.2 µg in 2013 and 10.9 µg in 2014. The sum of the absolute differences between IASI and MAN was somewhat larger in 2013, amounting to 7.9 µg, but considerably smaller in 2014, amounting to 6.0 µg.

	Month	LOTOS-EUROS				IASI-derived			
		r	slope	intercept	RMSD	r	slope	intercept	RMSD
MAN	04-2013	0.53 ↑	1.48	-1.41	4.33	0.46	1.05 ↑	-1.08 ↑	3.37 ↑
	05-2013	0.48 ↑	0.92 ↑	0.30	1.95 ↑	0.44	1.69	0.04 ↑	3.94
	06-2013	0.59	0.70 ↑	-0.06 ↑	2.66 ↑	0.59	1.42	-1.19	3.23
	07-2013	0.48 ↑	0.71	0.94	3.32 ↑	0.44	1.15 ↑	-0.06 ↑	4.18
	08-2013	0.49	0.89 ↑	1.67	3.37 ↑	0.49	1.15	1.11 ↑	4.03
	09-2013	0.40 ↑	1.45 ↑	0.15 ↑	3.47 ↑	0.25	3.05	-7.48	6.09
	04-2014	0.52 ↑	1.75	-2.80	5.66	0.35	0.98 ↑	-2.03 ↑	4.24 ↑
	05-2014	0.39	0.80	-0.10 ↑	2.78 ↑	0.46 ↑	1.08 ↑	-2.12	3.17
	06-2014	0.70	0.87 ↑	0.12 ↑	2.08 ↑	0.71 ↑	1.41	-1.44	2.74
	07-2014	0.56	0.76	0.18 ↑	2.74 ↑	0.56	1.08 ↑	-1.79	3.13
	08-2014	0.47	1.31 ↑	-0.57 ↑	2.44 ↑	0.47	1.50	-2.09	2.58
	09-2014	0.28 ↑	1.22 ↑	3.42 ↑	6.03 ↑	0.12	1.87	-3.73	6.23

Table 4: Month by month comparison of the correlation coefficient (r), slope and intercept of the monthly mean NH_3 surface concentrations of the MAN stations (x-axis) and the coinciding monthly mean LOTOS-EUROS and IASI-derived NH_3 surface concentrations (y-axis). The green arrows denote which of the two (LOTOS-EUROS or IASI) gives the most desirable values. The green arrows are attributed to either LOTOS-EUROS or IASI based on the following criteria: highest r, slope closest to 1, intercept closest to 0 and smallest RMSD.

Table 4 shows the correlation coefficient, the slope and the intercept of the MAN measurements versus the modelled and IASI-derived concentrations for the warm months in 2013 and 2014. In 2013, the IASI-derived concentrations show a weaker correlation with the MAN measurements than the modelled concentrations in all months. Only in May and June in 2014, the IASI-derived concentrations compared slightly better to the MAN measurements than the modelled concentrations.
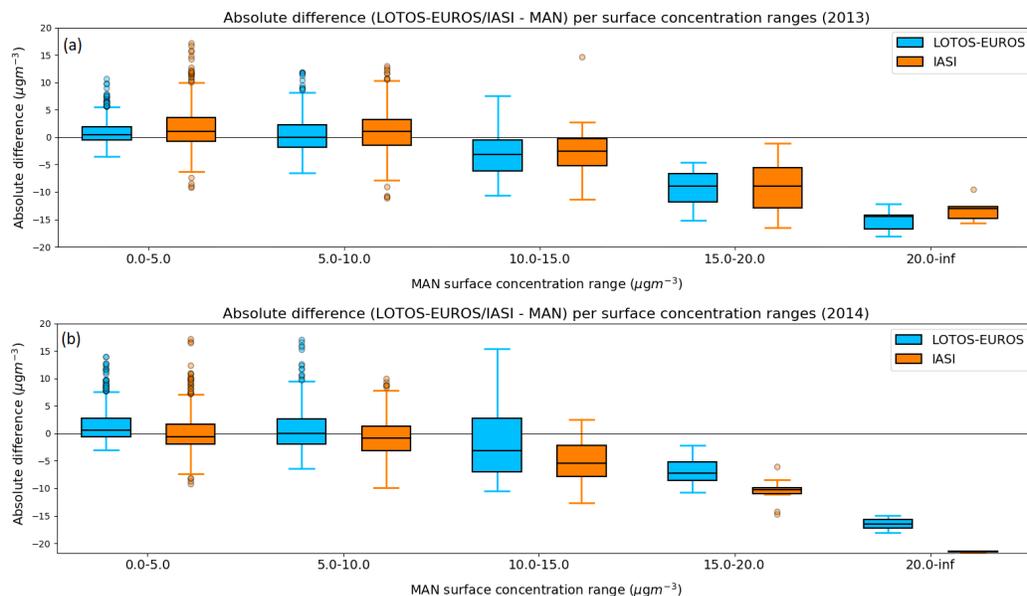
Figure 11: The absolute differences between the monthly mean NH$_3$ surface concentrations modelled in LOTOS-EUROS (blue) and derived from IASI (orange) and the monthly mean NH$_3$ surface concentrations measured by the MAN stations in the warm season (April-September) in 2013 (a) and 2014 (b), grouped as function of the MAN monthly mean NH$_3$ surface concentrations. The black line indicates the median, the edges of the boxes indicate the 25th and the 75th percentiles (Q1 and Q2), the whiskers indicate the full range of the absolute differences (Q1 – 1.5*IQR and Q3 + 1.5*IQR) and the dots indicate the outliers values that lie outside the whiskers.

The data is grouped into different MAN NH$_3$ surface concentration ranges to test the performance of the modelled and IASI-derived concentrations as a function of concentration level. Figure 11 shows the grouped absolute differences between the monthly mean NH$_3$ surface concentrations measured by the MAN stations and the corresponding modelled (blue) and IASI-derived (orange) concentrations. For low MAN concentration ranges (0-10 µgm^{-3}) the modelled concentrations agree fairly well with the MAN measurements in both years. For higher MAN concentration ranges (>10 µgm^{-3}) the model seems to underestimate the monthly mean NH$_3$ surface concentrations. The IASI-derived concentrations were relatively higher than the modelled concentrations for all concentration levels in 2013. The opposite is true in 2014, where the IASI-derived concentrations were relatively lower than the modelled concentrations. We conclude that the differences between modelled and IASI-derived concentrations in the Netherlands cannot be assigned to specific concentration levels.

In summary, the comparison with the MAN measurements does also not show any significant or consistent improvement in the IASI-derived concentrations compared to the modelled concentrations.

4.1.3   Summary of the comparison with in-situ measurements

We compared the modelled and IASI-derived concentrations to measurements of the European EMEP network. The IASI-derived concentrations showed in general a slightly stronger correlation with the EMEP measurements than modelled concentrations on a monthly basis. Moreover, the correlation became more pronounced on a seasonal basis

20

(mean of April-September). We then compared the modelled and the IASI-derived concentrations to measurements of Dutch MAN and LML networks. This comparison, on the other hand, did not show any significant or consistent improvement in the IASI-derived concentrations compared to the modelled concentrations.

5   In general, both the modelled and the IASI-derived concentrations seem to be overestimated in emission areas. This could potentially be related to the overpass time of the satellite. In high emission areas, the NH_3 concentrations are more variable in time, and the IASI observations might have an uncertain representativeness. Moreover, the measurements in high emission areas are generally more uncertain with regard to their spatial representativeness. Overall, these measurements can be more affected by local rather than regional sources.

10 Generally, the modelled and the observed NH_3 total columns match quite well. This means that the LOTOS-EUROS model represents the spatial distribution of NH_3 rather well. There are some areas with large discrepancies between the two where we see considerable deviations in the modelled and the IASI-derived concentrations. Most of these areas, however, cannot be validated against measurements, because of the lack of measurements here. The changes in the comparison of the available measurements with modelled versus IASI-derived concentrations are therefore

15 relativity small. Based on the measurements we have, we conclude that we do not see any significant improvement in the IASI-derived concentrations compared to the modelled concentrations.

The differences between Europe and the Netherlands could be explained by the location of the ground measurements. The majority of the European scale stations are located in background regions, with relatively well-

20 mixed and low NH_3 concentrations. Most stations in the Netherlands, on the other hand, are located in, or nearby, regions with relatively higher NH_3 concentrations. As a result, the vertical profile shapes in LOTOS-EUROS in the Netherlands are more complex and variable in time, as this region is influenced by a constantly changing combination of transport, emission and deposition. The use of an inadequate vertical profile to derive NH_3 surface concentrations from IASI could lead to an erroneous redistribution of the total amount of measured NH_3, therewith

25 worsening the comparability with in-situ measurements. On the contrary, the vertical profile shapes in background regions are more stable and constant in time, and therefore more likely to be described adequately by the LOTOS-EUROS model.

4.1.3.1   Side-note on validation with in-situ measurements

30 The differences between the in-situ measurement and the modelled and IASI-derived concentrations can partially be explained by their discrepancy in terms of spatial representation, which limits their comparability to some extent. The footprint of the in-situ measurements is relatively small and easily influenced by local factors, whereas the model and the satellite provide us with a mean value over a much larger area. The two high concentration stations of the LML network in the Netherlands, Vredepeel and Wekerom, are for instance influenced by nearby emission

35 sources which cannot be resolved by regional models at the current resolution.

4.2 NH_3 dry deposition flux

4.2.1 Europe

The monthly mean dry NH$_3$ deposition flux has been computed for the warm season (April to September) in 2013 and 2014. Figure 12 shows the warm season mean dry NH$_3$ deposition flux (kg N ha^{-1}yr^{-1}). The left figures show the original, modelled flux from LOTOS-EUROS (which will be referred to as the 'modelled flux'). The right figures show the modelled flux adjusted by the IASI satellite observations (which will be referred to as 'IASI-derived flux'). The modelled fluxes were very similar in both years. Figure 13 shows the absolute and relative differences between the modelled and the IASI-derived flux. In 2013, the IASI-derived fluxes were higher than the modelled fluxes in the Netherlands and Belgium. This depicts that the IASI-observed NH$_3$ total columns here were higher than the modelled total columns in LOTOS-EUROS. The IASI-derived fluxes were higher than the modelled fluxes in other areas such as Germany, and large parts of Central Europe, mainly in Poland, Belarus and Romania. In 2014, the IASI-derived fluxes were much higher than the modelled flux in parts of Central Europe, mainly in Poland and the Czech Republic, and in parts of the United Kingdom, for instance North-Ireland. In both years, the IASI-derived fluxes were much lower than modelled fluxes in Switzerland, the Po Valley in Italy and the northern part of Turkey. Here, the IASI-observed NH$_3$ total columns were thus consistently lower than the modelled total columns in LOTOS-EUROS. Inadequate emission input data could explain the differences at these locations. Another possible cause is incorrect modelling of the atmospheric transport and/or stability of NH$_3$ in LOTOS-EUROS.
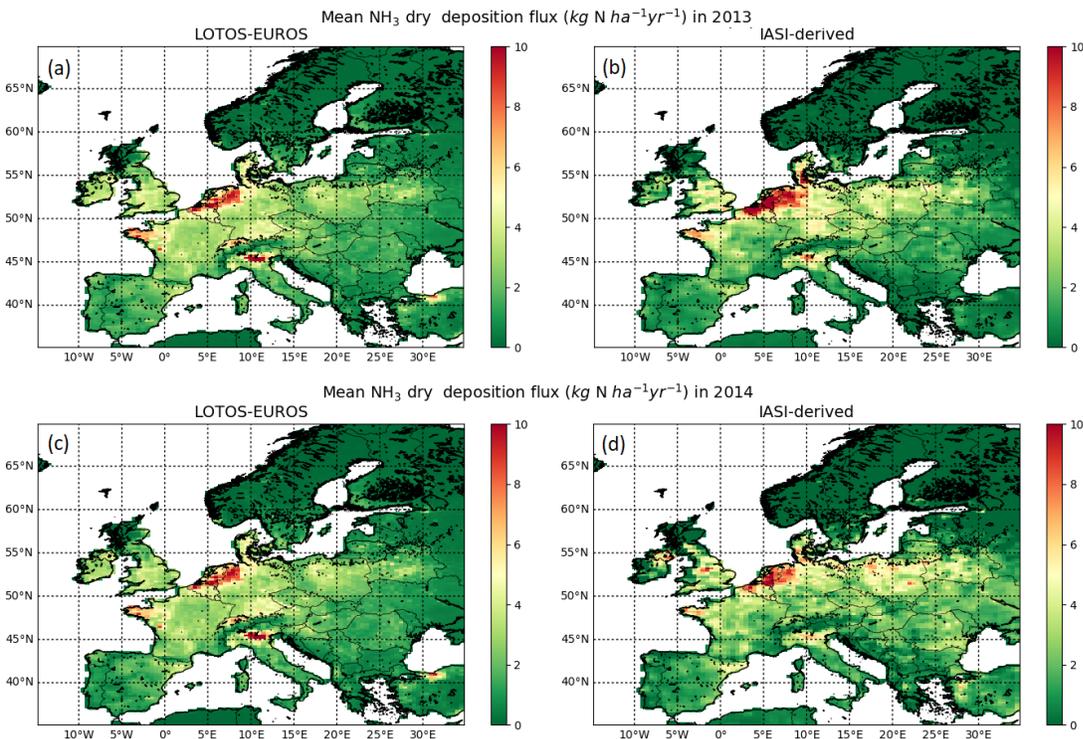

Figure 12: The warm season (April to September) mean NH$_3$ dry deposition modelled in LOTOS-EUROS (left) and inferred from IASI (right) in kg N ha^{-1}yr^{-1} in 2013 (top) and 2014 (bottom).

Absolute difference (IASI-derived - LOTOS-EUROS) in mean NH$_3$ dry deposition flux (kg N $ha^{-1}yr^{-1}$)
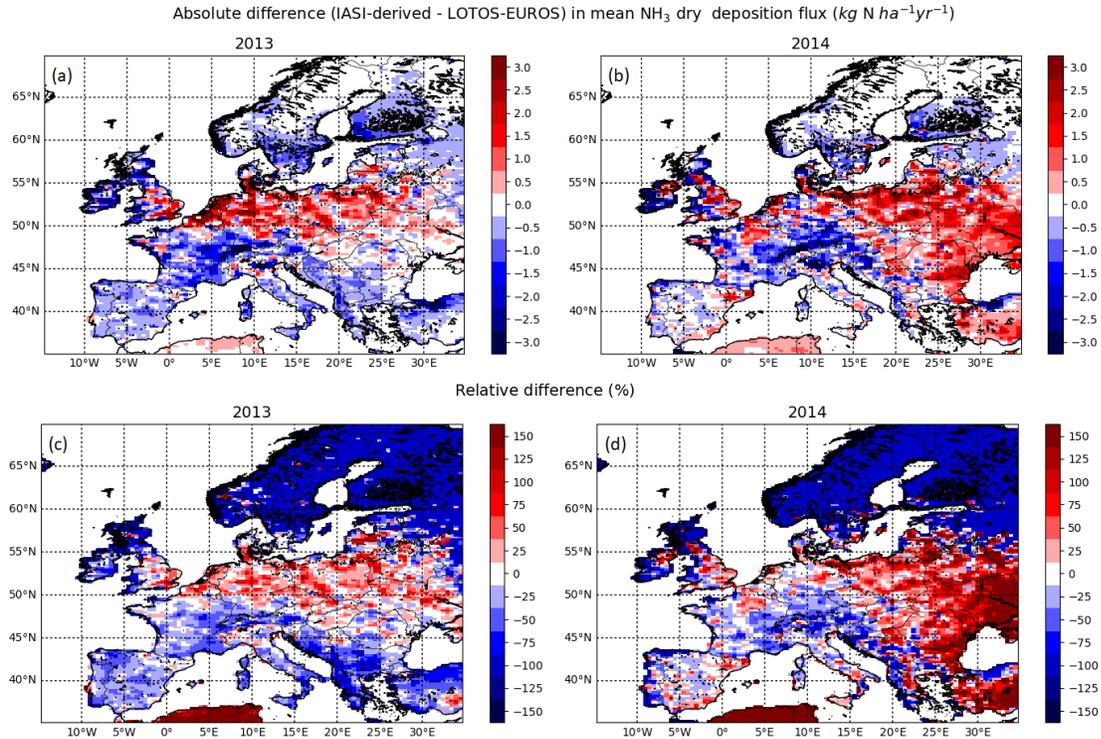

Figure 13: The absolute (top) and relative (bottom) differences in the warm season (April to September) mean NH$_3$ dry deposition modelled in LOTOS-EUROS and inferred from IASI in 2013 (left) and 2014 (right).

4.2.2   The Netherlands

5   The modelled and IASI-derived fluxes in the Netherlands are shown in Figure 14. Figure 14 shows that the modelled fluxes were similar in both years, whereas the IASI-derived flux varied quite a lot. The IASI-derived flux is higher than the modelled flux in 2013, and lower than the modelled flux in 2014. The IASI-observed NH$_3$ total columns in the Netherlands were thus in general somewhat higher than the modelled NH$_3$ columns in 2013, and somewhat lower than the modelled NH$_3$ columns in 2014.
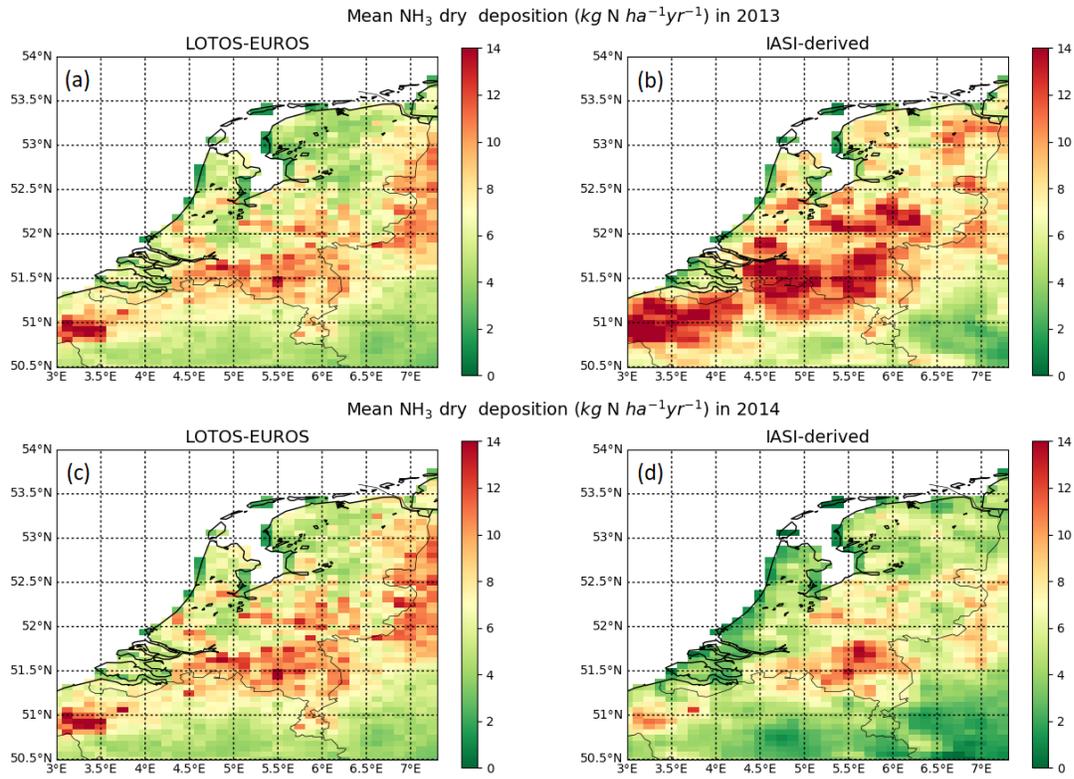
Figure 14: The warm season (April to September) mean NH₃ dry deposition in the Netherlands modelled in LOTOS-EUROS (left) and inferred from IASI (right) in kg N ha⁻¹yr⁻¹ in 2013 (top) and 2014 (bottom).

Absolute differences (IASI-derived - LOTOS-EUROS) in NH$_3$ dry deposition flux (kg N $ha^{-1}yr^{-1}$)
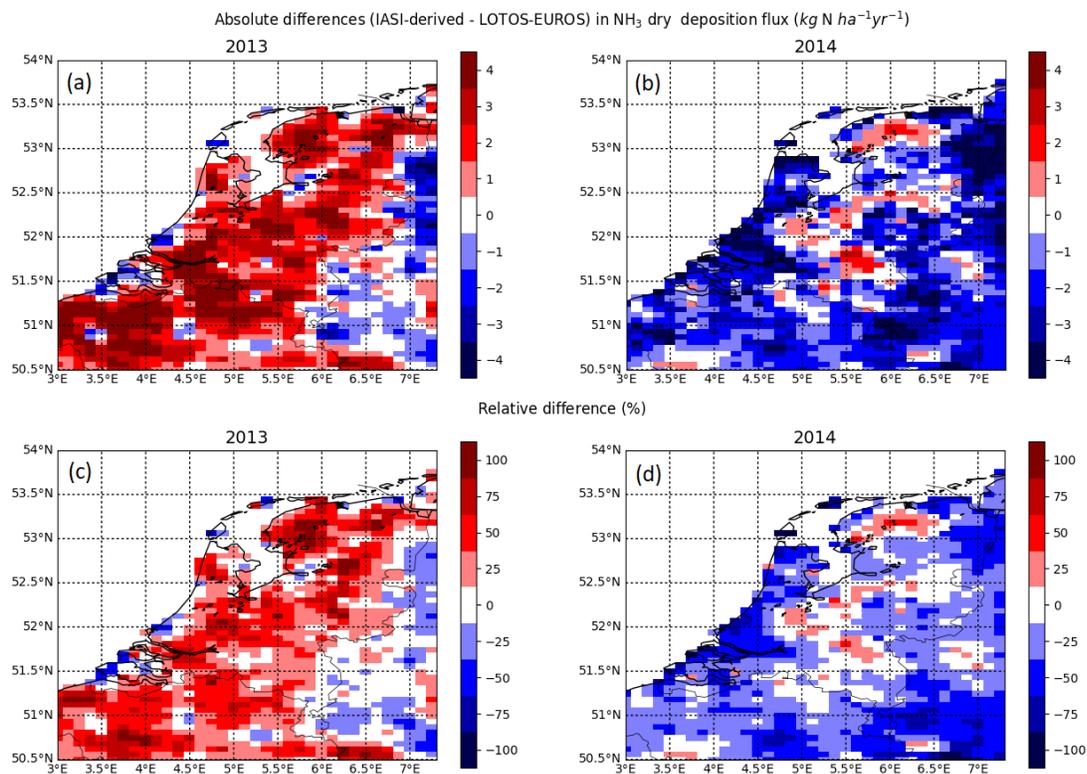
Relative difference (%)

Figure 15: The absolute (top) and relative (bottom) differences in the warm season (April to September) mean NH$_3$ dry deposition in the Netherlands modelled in LOTOS-EUROS and inferred from IASI in 2013 (left) and 2014 (right).

Figure 15 depicts the absolute and relative differences between the modelled and IASI-derived fluxes. In 2013, the main differences occur in the central and northernmost parts of the Netherlands, where the IASI-derived fluxes are clearly higher than the modelled ones. Furthermore, the IASI-derived fluxes are higher than the modelled fluxes for the largest part of the Netherlands. In 2014, the IASI-derived fluxes are lower than the modelled fluxes for the largest part of the Netherlands, except for the center and the northernmost part.

4.2.3 Inter-annual differences

The inter-annual variations of the modelled and IASI-derived flux differences (see Figure 13 and 15) could be related to different meteorological conditions. The annual global climate reports from the NOAA (National Oceanic and Atmosphere Administration) show that the mean temperatures in Europe were higher in 2014 than in 2013, especially in western Europe. This might have had an effect on the actual emissions and their variability, which is only limited taken into account by the model. The annual precipitation in both years was near average for Europe as a whole. However, if we zoom in to a more regional scale, we see that it was much wetter than average during the warm season in nearly all parts of the Balkan Peninsula and Turkey (NOAA, 2014, 2015). Figure 13 shows that the largest inter-annual variations on a European scale occur around the Black Sea: in Ukraine, but also in the eastern parts of the Balkan Peninsula and Turkey. Some of these regions thus coincide with regions that experienced heavy rainfall in 2014 and might have affected emission and deposition processes which are not taken into account by the

model. This suggests that meteorological effects might indeed influence our results. However, the examined period of two warm seasons only is too short to draw a conclusion.

4.3. LOTOS-EUROS sensitivity study

The results of the sensitivity runs are summarized in Figure 16, 17 and 18. Figure 16 shows the relative changes in the warm season mean terrestrial dry NH_3 deposition flux over Europe modelled in LOTOS-EUROS (a) and derived from IASI (b) in 2014 for different model runs. The mean LOTOS-EUROS dry NH_3 deposition over the land cells in the modelling grid in 2014 was 1.76 kg N ha^{-1} yr^{-1}. The mean IASI-derived dry NH_3 deposition flux was somewhat higher, namely 2.20 kg N ha^{-2} yr^{-1}.

Variations in the MACC-III NH_3 emissions caused the largest changes in the modelled flux. The smallest change was obtained by variation of the wet deposition scavenging coefficient G_{scav}. The variations in the dry deposition velocity V_d led to the biggest changes in the IASI-derived flux. The effect appears to be amplified compared to the effect on the modelled flux. The effect of the MACC-III NH_3 emissions is damped. On the other hand, the effect of the MACC-III NO_X and SO_2 emissions is also amplified. The signs of the changes in the IASI-derived flux have flipped because of the changes in MACC-III NH_3, MACC-III NO_X and SO_2 and G_{scav}. The modelled flux is one to one sensitive to emission changes in NH_3, whereas for IASI-derived flux this is much less. The IASI-derived flux, in turn, changes one to one with the V_d.

The variations in the modelled flux are a result of daily and monthly variations in emissions. The variations in the IASI-derived flux are also a result of these variations, but on top of this also include an effect of the overpass time of the satellite.
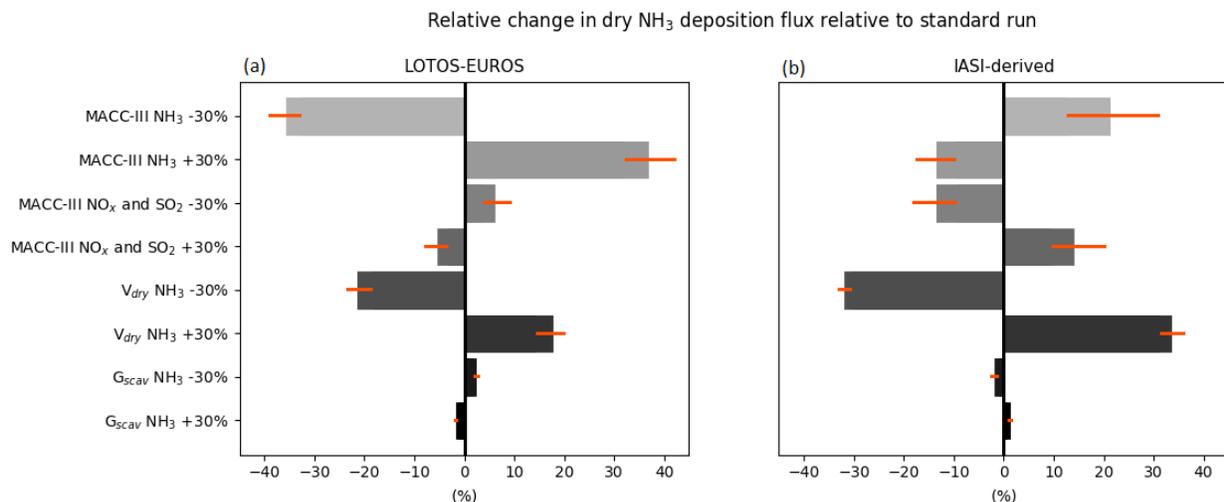
Figure 16: The median change (%) in the terrestrial NH_3 dry deposition flux in 2014 in (kg N ha^{-1} yr^{-1}) from LOTOS-EUROS (a) and IASI-derived (b), resulting from different perturbations of model inputs of LOTOS-EUROS. The orange lines indicate the 25th and the 75th quartiles.
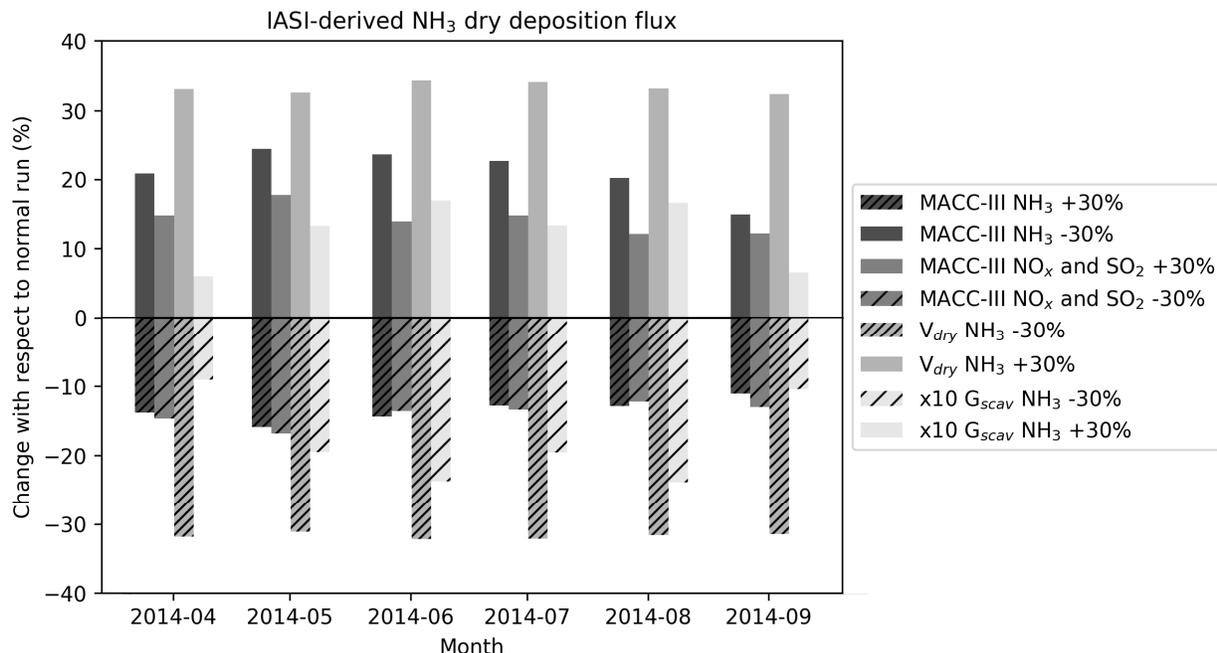
Figure 17: The change (%) in the monthly mean IASI-derived NH$_3$ dry deposition flux resulting from different perturbations of the LOTOS-EUROS model.

Figure 17 shows the changes (%) of monthly mean IASI-derived fluxes in 2014 resulting from the different LOTOS-EUROS sensitivity runs. Note that the effect of the runs with changes in wet deposition through variations of the gas scavenging coefficient for NH$_3$ is enlarged by a factor 10. We see that the changes with respect to the standard LOTOS-EUROS run are in general constant over the months. The least variation is observed for the runs with changed V$_{dry}$ values, that all resulted in a change of ~31% per month. The runs with adjusted MACC-III emissions of NH$_3$ and emissions of NO$_x$ and SO$_2$ led to largest changes in May and the smallest changes in September. The maximum difference between months is 9.5% and 5.6%, respectively, for the runs with adjusted NH$_3$ and the runs with adjusted NO$_x$ and SO$_2$ values. The runs with changed values of G$_{scav}$ for NH$_3$ seem to be affected most by changing weather conditions, which resulted in the relatively largest variation per month. However, because the changes in the IASI-derived flux are small (-2.4 to +1.7%), we now continue to look at yearly changes.
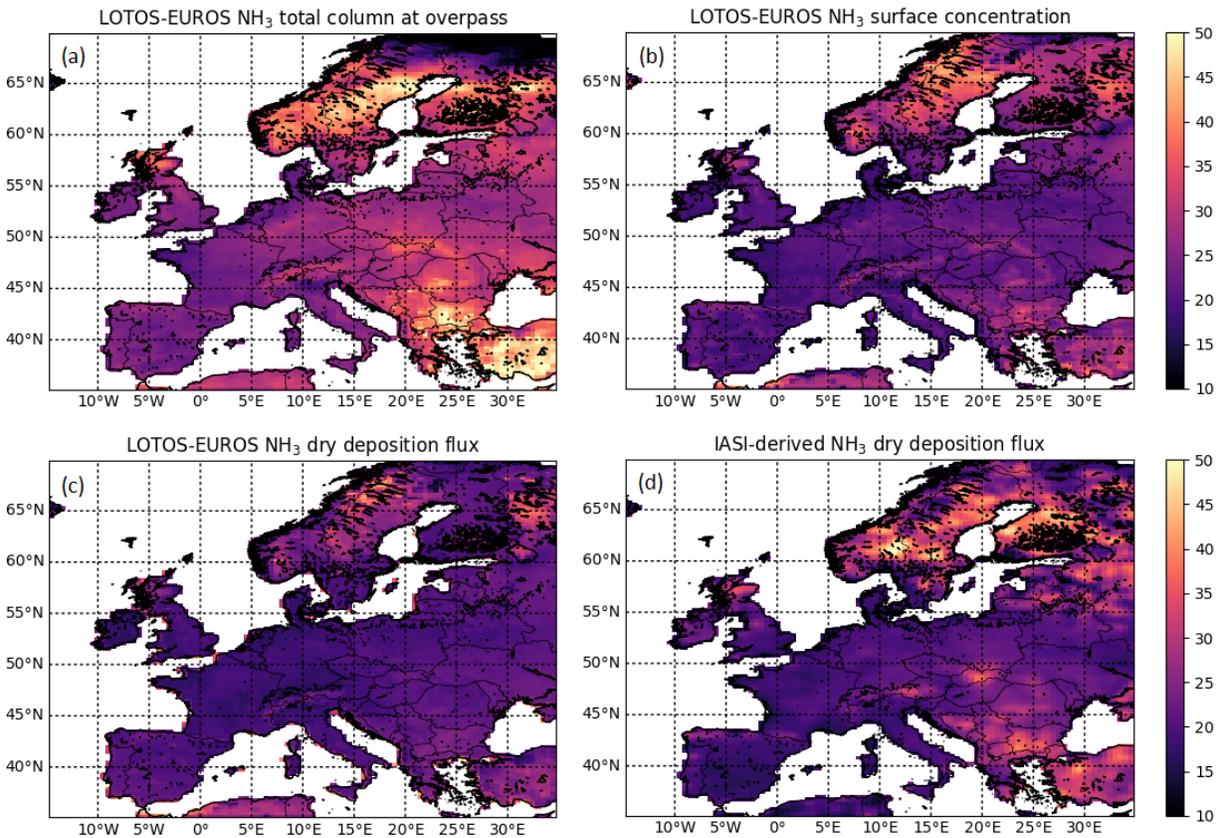
Figure 18: The relative standard deviation (%) of the warm season mean output of all perturbed runs and the associated dry deposition estimate inferred from IASI in 2014. Figure (a) shows the LOTOS-EUROS NH$_3$ total column concentration at overpass time, (b) the LOTOS-EUROS NH$_3$ surface concentration, (c) the NH$_3$ dry deposition flux in LOTOS-EUROS and (d) the resulting IASI-derived NH$_3$ dry deposition flux.

Figure 18 shows the relative standard deviation (%) of all 8 sensitivity runs for Europe. The bottom-right figure (d) shows the relative standard deviation of the final IASI-derived flux. The relative standard deviation varies from ~20% to ~50% throughout Europe. The smallest variations can be seen in the southwestern and central parts of Europe. The highest variations, of ~40 - 50%, are mainly found in long-distance transport areas with low NH$_3$ concentrations and deposition fluxes, such as Scandinavia, and in areas with high aerosol precursor emissions, such as the Balkans.

5. Discussion

In this paper, we examined the applicability and the limitations of the method suggested by Nowlan et al. (2014) for the derivation of NH$_3$ surface concentrations and dry deposition fluxes across Europe. A comparison of the LOTOS-EUROS modelled and IASI-derived NH$_3$ surface concentrations with in-situ measurements of the EMEP network on a European scale and the LML and MAN network in the Netherlands has been made. Although there appeared to be some improvements in the IASI-derived NH$_3$ surface concentrations compared to the modelled LOTOS-EUROS

NH$_3$ surface concentrations, mainly in background regions, there did not seem to be any significant, consistent improvement. In addition, the timing of the IASI-derived NH$_3$ surface concentrations did not show better correspondence with the in-situ observations than the modelled NH$_3$ surface concentrations. Consequently, as the dry NH$_3$ deposition fluxes are directly derived from the NH$_3$ surface concentrations, no significant improvement is

5   expected here either. On top of this, the sensitivity study using eight input parameters important for NH$_3$ dry deposition modelling showed that the effect of model uncertainties on the IASI-derived dry NH$_3$ deposition fluxes is amplified by the estimation procedure compared to the effect on the model simulations itself. The final IASI-derived dry NH$_3$ deposition fluxes can vary ~20% up to ~50% throughout Europe as a result of model uncertainties.

The method used to derive the NH$_3$ surface concentrations and dry deposition fluxes from IASI observations is

10   based on various assumptions. For one, the method assumes that the relationship between the NH$_3$ concentration and the dry deposition flux is linear, whereas this relationship is in reality non-linear. In fact, these quantities can even be anti-correlated with highest surface concentrations during the night when the atmosphere is stable and the exchange is limited. The compensation point of NH$_3$ further enhances the non-linearity. For our purpose, focusing on a single time of the day using monthly data, however, approximating this concentration-flux relationship by a

15   linear curve may seem reasonable for concentration regimes below the saturation point. For higher NH$_3$ surface concentrations the current approach will likely lead to overestimated dry deposition fluxes. Moreover, this study includes the impact of the compensation point of NH$_3$ through the dry deposition scheme in LOTOS-EUROS. Although the uncertainties are relatively large as the used compensation points are based on relatively few observations (e.g. (Wichink Kruit et al., 2007)), we feel that the inclusion of the compensation point is a strong point

20   of this study.

Moreover, the approach by Nowlan also assumes that the NH$_3$ total column concentrations measured by IASI serve as a direct proxy of the NH$_3$ surface concentrations. In reality, however, the relationship between the two is influenced by various different factors, including the vertical distribution of NH$_3$ and the satellites sensitivity. There are already quite some uncertainties involved with the vertical distribution of NH$_3$ and therefore tower measurement

25   campaigns (Dammers et al., 2017a;Li et al., 2017a) are very important to strengthen our understanding. Dammers et al. (2017a) for instance showed that the daytime boundary layer is well mixed, which supports the choice of a model that uses the mixed layer approach such as LOTOS-EUROS. Li et al. (2017b) showed that there is a clear seasonal variation in the vertical distribution of NH$_3$ and that the slope of the NH$_3$ concentration gradient varies throughout the year. During winter, Li et al. (2017b) observed relatively high NH$_3$ ground concentrations due to potential

30   trapping of NH$_3$ emissions in a shallow winter boundary layer, and reduced NH$_3$ concentrations higher up the column. In these types of situations, the IASI-satellite instrument potentially misses high NH$_3$ ground concentrations because of the lack of sensitivity to the lower parts of the boundary layer. The computation of averaging kernels for IASI could help to indicate more precisely where the sensitivity lies and how the measured total columns are distributed. Moreover, further development and validation of the IASI retrieval may help to improve our

35   understanding of the satellites product, therewith also increasing its applicability.

The method also assumes that the timing and distribution of the emissions in the LOTOS-EUROS model closely represent reality, as the ratio between the retrieved and the modelled ammonia burden is used at overpass time. The accuracy of the seasonal variation in the NH_3 emissions in LOTOS-EUROS is therefore of great importance. The reliability of yearly dry NH_3 deposition estimates using our method is limited by the lack of high-quality IASI observations during the cold season. As a result, derivation of yearly IASI-derived NH_3 dry deposition estimates may differ substantially depending on whether or not the spring maximum peak occurs in the satellite-observed months (April – September). Skjøth et al. (2011) presented the seasonal variation and the distribution of NH_3 emissions for different European countries per agricultural source. They showed for instance that approximately half of the NH_3 emissions from spring fertilization are usually emitted in March. As the spring fertilization amounts to ~20-50% of the yearly total NH_3 emissions, this may result in a variation of the same magnitude on the subsequent deposition estimates. Improvement of the seasonal variation in NH_3 emissions in LOTOS-EUROS could be used to fill in this gap and lead to a more accurate representation of reality. Skjøth et al. (2011) showed that the implementation of a dynamic NH_3 emission model for different agricultural sources may result in considerable model performance improvements when high-quality activity data and information on spatial distributions of emissions is available. Furthermore, Hendriks et al. (2016) showed that the use of manure transport data for NH_3 emission time profiles leads to additional model improvements and a better representation of the spring maximum.

Moreover, mismatches between the actual and modelled diurnal variations in NH_3 emission could also easily lead to large differences in the IASI-derived dry NH_3 deposition estimates. As an illustration, Sintermann et al. (2016) for instance measured NH_3 emissions from an agricultural surface after slurry application and showed that ~80% of the total NH_3 was emitted within 2 hours. Combined with the short-lifetime of NH_3 there is a possibility that the IASI-instrument completely misses these kinds of events if they occur after its overpass. A possible way to reduce the impact of the diurnal variation is to combine information from IASI with other satellites that have different overpass times. NH_3 observations from the CrIS satellite instrument could, for instance, be used (Shephard and Cady-Pereira, 2015).

At this stage, we can conclude that the IASI-derived NH_3 deposition fluxes do not show strong improvements compared to modelled NH_3 deposition fluxes and there is a future need for better, more robust, methods to derive NH_3 dry deposition fluxes. This could potentially be achieved by further integration of existing in-situ- and satellite data into models with special attention to data representativeness, for instance by means of data-assimilation. In addition, there is a need for a better understanding of the surface exchange of NH_3 for different land use types. Model parameterizations of the surface exchange of NH_3 are now based on a limited number of direct flux measurements, and more measurements could definitely improve this. Also, a better understanding of the timing and distribution of NH_3 emissions could lead to considerable improvements in modelled emissions fields and consequently deposition fields from CTMs.

Acknowledgements

acknowledge the Aeris website (https://iasi.aeris-data.fr/nh3/) for providing access to the IASI-NH$_3$ dataset. Moreover, we would like to thank the RIVM and the EMEP for maintaining, collecting, and sharing data from their NH$_3$ ground networks.

References

5   Behera, S. N., Sharma, M., Aneja, V. P., and Balasubramanian, R.: Ammonia in the atmosphere: a review on emission sources, atmospheric chemistry and deposition on terrestrial bodies, Environ Sci Pollut Res Int, 20, 8092-8131, 10.1007/s11356-013-2051-9, 2013.

Bessagnet, B., Pirovano, G., Mircea, M., Cuvelier, C., Aulinger, A., Calori, G., Ciarelli, G., Manders, A., Stern, R., Tsyro, S., García Vivanco, M., Thunis, P., Pay, M.-T., Colette, A., Couvidat, F., Meleux, F., Rouïl, L., Ung, A.,
10   Aksoyoglu, S., Baldasano, J. M., Bieser, J., Briganti, G., Cappelletti, A., D'Isodoro, M., Finardi, S., Kranenburg, R., Silibello, C., Carnevale, C., Aas, W., Dupont, J.-C., Fagerli, H., Gonzalez, L., Menut, L., Prévôt, A. S. H., Roberts, P., and White, L.: Presentation of the EURODELTA III inter-comparison exercise – Evaluation of the chemistry transport models performance on criteria pollutants and joint analysis with meteorology, Atmos. Chem. Phys. Discuss, 16, 10.5194/acp-16-12667-2016, 2016.

15   Blank, F. T.: Meetonzekerheid Landelijk Meetnet Luchtkwaliteit (LML), KEMA, 50050870-KPS/TCM 01-3063, 2001.

Clerbaux, C., Boynard, A., Clarisse, L., George, M., Hadji-Lazaro, J., Herbin, H., Hurtmans, D., Pommier, M., Razavi, A., Turquety, S., Wespes, C., and Coheur, P. F.: Monitoring of atmospheric composition using the thermal infrared IASI/MetOp sounder, Atmos Chem Phys, 9, 6041-6054, 2009.

20   Colette, A., Andersson, C., Manders, A., Mar, K., Mircea, M., Pay, M. T., Raffort, V., Tsyro, S., Cuvelier, C., Adani, M., Bessagnet, B., Bergstrom, R., Briganti, G., Butler, T., Cappelletti, A., Couvidat, F., D'Isidoro, M., Doumbia, T., Fagerli, H., Granier, C., Heyes, C., Klimont, Z., Ojha, N., Otero, N., Schaap, M., Sindelarova, K., Stegehuis, A. I., Roustan, Y., Vautard, R., van Meijgaard, E., Vivanco, M. G., and Wind, P.: EURODELTA-Trends, a multi-model experiment of air quality hindcast in Europe over 1990-2010, Geosci Model Dev, 10, 3255-3276,
25   10.5194/gmd-10-3255-2017, 2017.

Dammers, E., Palm, M., Van Damme, M., Vigouroux, C., Smale, D., Conway, S., Toon, G. C., Jones, N., Nussbaumer, E., Warneke, T., Petri, C., Clarisse, L., Clerbaux, C., Hermans, C., Lutsch, E., Strong, K., Hannigan, J. W., Nakajima, H., Morino, I., Herrera, B., Stremme, W., Grutter, M., Schaap, M., Kruit, R. J. W., Notholt, J., Coheur, P. F., and Erisman, J. W.: An evaluation of IASI-NH3 with ground-based Fourier transform infrared
30   spectroscopy measurements, Atmos Chem Phys, 16, 10351-10368, 10.5194/acp-16-10351-2016, 2016.

Dammers, E., Schaap, M., Haaima, M., Palm, M., Kruit, R. J. W., Volten, H., Hensen, A., Swart, D., and Erisman, J. W.: Measuring atmospheric ammonia with remote sensing campaign: Part 1-Characterisation of vertical ammonia

concentration profile in the centre of The Netherlands, Atmos Environ, 169, 97-112, 10.1016/j.atmosenv.2017.08.067, 2017a.

Dammers, E., Shephard, M. W., Palm, M., Cady-Pereira, K., Capps, S., Lutsch, E., Strong, K., Hannigan, J. W., Ortega, I., Toon, G. C., Stremme, W., Grutter, M., Jones, N., Smale, D., Siemons, J., Hrpcek, K., Tremblay, D., Schaap, M., Notholt, J., and Erisman, J. W.: Validation of the CrIS fast physical NH3 retrieval with ground-based FTIR, Atmos Meas Tech, 10, 2645-2667, 10.5194/amt-10-2645-2017, 2017b.

Denier van der Gon, H. A. C., Hendriks, C., Kuenen, J., Segers, A., and Visschedijk, A.: Description of current temporal emission patterns and sensitivity of predicted AQ for temporal emission patterns., TNO Report, 2011.

Dentener, F., Drevet, J., Lamarque, J. F., Bey, I., Eickhout, B., Fiore, A. M., Hauglustaine, D., Horowitz, L. W., Krol, M., Kulshrestha, U. C., Lawrence, M., Galy-Lacaux, C., Rast, S., Shindell, D., Stevenson, D., Van Noije, T., Atherton, C., Bell, N., Bergman, D., Butler, T., Cofala, J., Collins, B., Doherty, R., Ellingsen, K., Galloway, J., Gauss, M., Montanaro, V., Muller, J. F., Pitari, G., Rodriguez, J., Sanderson, M., Solmon, F., Strahan, S., Schultz, M., Sudo, K., Szopa, S., and Wild, O.: Nitrogen and sulfur deposition on regional and global scales: A multimodel evaluation, Global Biogeochem Cy, 20, Artn Gb4003 10.1029/2005gb002672, 2006a.

Dentener, F., Stevenson, D., Ellingsen, K., van Noije, T., Schultz, M., Amann, M., Atherton, C., Bell, N., Bergmann, D., Bey, I., Bouwman, L., Butler, T., Cofala, J., Collins, B., Drevet, J., Doherty, R., Eickhout, B., Eskes, H., Fiore, A., Gauss, M., Hauglustaine, D., Horowitz, L., Isaksen, I. S. A., Josse, B., Lawrence, M., Krol, M., Lamarque, J. F., Montanaro, V., Muller, J. F., Peuch, V. H., Pitari, G., Pyle, J., Rast, S., Rodriguez, J., Sanderson, M., Savage, N. H., Shindell, D., Strahan, S., Szopa, S., Sudo, K., Van Dingenen, R., Wild, O., and Zeng, G.: The global atmospheric environment for the next generation, Environ Sci Technol, 40, 3586-3594, 10.1021/es0523845, 2006b.

ECMWF: European Centre for Medium-Range Weather Forecasts Annual report, 2016.

EEA: European Union emission inventory report 1990–2014 under the UNECE Convention on Long-range Transboundary Air Pollution (LRTAP), EEA Report, 16, 10.2800/628267, 2016.

EMEP: The European Monitoring and Evaluation Programme EMEP Status Report, 2016.

Erisman, J. W.: Acid deposition to nature areas in the Netherlands: Part I Methods and results, Water Air Soil Poll, 71, 51-80, 1993.

Erisman, J. W., and Draaijers, G. P. J.: Atmospheric deposition in relation to acidification and eutrophication, Elsevier 1995.

Erisman, J. W., Sutton, M. A., Galloway, J., Klimont, Z., and Winiwarter, W.: How a century of ammonia synthesis changed the world, Nat Geosci, 1, 636-639, 10.1038/ngeo325, 2008.

Erisman, J. W., Galloway, J., Dice, N. B., Sutton, M., Bleeker, A., Grizzetti, B., Leach, A., and de Vries, W.: Nitrogen: too much of a vital resource, Science Brief. , WWF Netherlands, Zeist, The Netherlands, 2015.

5 Flechard, C. R., Nemitz, E., Smith, R. I., Fowler, D., Vermeulen, A. T., Bleeker, A., Erisman, J. W., Simpson, D., Zhang, L., Tang, Y. S., and Sutton, M. A.: Dry deposition of reactive nitrogen to European ecosystems: a comparison of inferential models across the NitroEurope network, Atmos Chem Phys, 11, 2703-2728, 10.5194/acp-11-2703-2011, 2011.

Fowler, D., Coyle, M., Skiba, U., Sutton, M. A., Cape, J. N., Reis, S., Sheppard, L. J., Jenkins, A., Grizzetti, B.,
10 Galloway, J. N., Vitousek, P., Leach, A., Bouwman, A. F., Butterbach-Bahl, K., Dentener, F., Stevenson, D., Amann, M., and Voss, M.: The global nitrogen cycle in the twenty-first century, Philos T R Soc B, 368, ARTN 20130164 10.1098/rstb.2013.0164, 2013.

Galloway, J. N., Aber, J. D., Erisman, J. W., Seitzinger, S. P., Howarth, R. W., Cowling, E. B., and Cosby, B. J.: The nitrogen cascade, Bioscience, 53, 341-356, Doi 10.1641/0006-3568(2003)053[0341:Tnc]2.0.Co;2, 2003.

15 Hendriks, C., Kranenburg, R., Kuenen, J. J. P., Van den Bril, B., Verguts, V., and Schaap, M.: Ammonia emission time profiles based on manure transport data improve ammonia modelling across north western Europe, Atmos Environ, 131, 83-96, 10.1016/j.atmosenv.2016.01.043, 2016.

Kharol, S. K., Shephard, M. W., McLinden, C. A., Zang, L., Sioris, C. E., O'Brien, J. M., Vet, R., Cady-Pereira, K. E., Hare, E., Siemons, J., and Krotkov, N. A.: Dry deposition of reactive nitrogen from satellite observations of
20 ammonia and nitrogen dioxide over North America, Geophys Res Lett, 10.1002/2017GL075832, 2017.

Kuenen, J. J. P., Visschedijk, A. J. H., Jozwicka, M., and van der Gon, H. A. C. D.: TNO-MACC_II emission inventory; a multi-year (2003-2009) consistent high-resolution European emission inventory for air quality modelling, Atmos Chem Phys, 14, 10963-10976, 10.5194/acp-14-10963-2014, 2014.

Li, Y., Thompson, T. M., Van Damme, M., Chen, X., Benedict, K. B., Shao, Y., Day, D., Boris, A., Sullivan, A. P.,
25 Ham, J., Whitburn, S., Clarisse, L., Coheur, P.-F., and Collett Jr., J. L.: Temporal and spatial variability of ammonia in urban and agricultural regions of northern Colorado, United States, Atmos Chem Phys, 17, 6197-6213, https://doi.org/10.5194/acp-17-6197-2017, 2017a.

Li, Y., Thompson, T. M., Van Damme, M., Chen, X., Benedict, K. B., Shao, Y. X., Day, D., Boris, A., Sullivan, A. P., Ham, J., Whitburn, S., Clarisse, L., Coheur, P. F., and Collett, J. L.: Temporal and spatial variability of ammonia
30 in urban and agricultural regions of northern Colorado, United States, Atmos Chem Phys, 17, 6197-6213, 10.5194/acp-17-6197-2017, 2017b.

Lolkema, D. E., Noordijk, H., Stolk, A. P., Hoogerbrugge, R., van Zanten, M. C., and van Pul, W. A. J.: The Measuring Ammonia in Nature (MAN) network in the Netherlands, Biogeosciences, 12, 5133-5142, 10.5194/bg-12-5133-2015, 2015.

Manders, A. M. M., Builtjes, P. J. H., Curier, L., Denier van der Gon, H. A. C., Hendriks, C., Jonkers, S., Kranenburg, R., Kuenen, J., Segers, A. J., Timmermans, R. M. A., Visschedijk, A., Wichink Kruit, R. J., Van Pul, W. A. J., Sauter, F. J., van der Swaluw, E., Swart, D. P. J., Douros, J., Eskes, H., van Meijgaard, E., van Ulft, B., van Velthoven, P., Banzhaf, S., Mues, A., Stern, R., Fu, G., Lu, S., Heemink, A., van Velzen, N., and Schaap, M.: Curriculum vitae of the LOTOS–EUROS (v2.0) chemistry transport model, Geosci Model Dev, 10(11), 10.5194/gmd-10-4145-2017, 2017.

National Centers for Environmental Information: State of the Climate: Global Climate Report for Annual 2013., access: January 10, 2014.

National Centers for Environmental Information: State of the Climate: Global Climate Report for Annual 2014., access: January 10, 2015.

Nowlan, C. R., Martin, R. V., Philip, S., Lamsal, L. N., Krotkov, N. A., Marais, E. A., Wang, S., and Zhang, Q.: Global dry deposition of nitrogen dioxide and sulfur dioxide inferred from space-based measurements, Global Biogeochem Cy, 28, 1025-1043, 10.1002/2014gb004805, 2014.

Reis, S., Pinder, R. W., Zhang, M., Lijie, G., and Sutton, M. A.: Reactive nitrogen in atmospheric emission inventories, Atmos Chem Phys, 9, 7657-7677, 10.5194/acp-9-7657-2009, 2009.

http://www.lml.rivm.nl/.

Schaap, M., Manders, A., Hendricks, J. M., Cnossen, A. J. S., Segers, H. A. C., Denier van der Gon, M., Jozwicka, M., Sauter, F., Velders, G., Matthijsen, J., and Builtjes, P.: Regional modelling of particulate matter for the Netherlands, Netherlands Research Program on Particulate Matter, 500099008, 2009.

Schrader, F., and Brummer, C.: Land Use Specific Ammonia Deposition Velocities: a Review of Recent Studies (2004-2013), Water Air Soil Poll, 225, ARTN 2114 10.1007/s11270-014-2114-7, 2014.

Shephard, M. W., and Cady-Pereira, K. E.: Cross-track Infrared Sounder (CrIS) satellite observations oftropospheric ammonia, Atmos. Meas. Tech., 8, 1323–1336, 10.5194/amt-8-1323-2015, 2015.

Sintermann, J., Dietrich, K., Hani, C., Bell, M., Jocher, M., and Neftel, A.: A miniDOAS instrument optimised for ammonia fieldmeasurements, Atmos Meas Tech, Discussions, doi:10.5194/amt-2015-360, 2016.

Skjøth, C. A., Geels, C., Berge, H., Gyldenkærne, S., Fagerli, H., Ellermann, T., Frohn, L. M., Christensen, J., Hansen, K. M., Hansen, K., and Hertel, O.: Spatial and temporal variation in ammonia emissions - a freely accessible model code for Europe Atmos Chem Phys, 11, 5221-5236, 10.5194/acp-11-5221-2011, 2011.

Spindler, G., Teichmann, U., and Sutton, M. A.: Ammonia dry deposition over grassland-micrometeorological flux-gradient measurements and bidirectional flux calculations using an inferential model, Q J Roy Meteor Soc, 127, 795 - 814, 10.1002/qj.49712757305, 2001.

Tørseth, K., Aas, W., Breivik, K., Fjæraa, A. M. F., M., Hjellbrekke, A. G., Lund Myhre, C., Solberg, S., and Yttri, K. E.: Introduction to the European Monitoring and Evaluation Programme (EMEP) and observed atmospheric composition change during 1972–2009, Atmos Chem Phys, 12, 5447-5481, https://doi.org/10.5194/acp-12-5447-2012, 2012.

Van Damme, M., Clarisse, L., Heald, C. L., Hurtmans, D., Ngadi, Y., Clerbaux, C., Dolman, A. J., Erisman, J. W., and Coheur, P. F.: Global distributions, time series and error characterization of atmospheric ammonia (NH3) from IASI satellite observations, Atmos Chem Phys, 14, 2905-2922, 10.5194/acp-14-2905-2014, 2014a.

Van Damme, M., Kruit, R. J. W., Schaap, M., Clarisse, L., Clerbaux, C., Coheur, P. F., Dammers, E., Dolman, A. J., and Erisman, J. W.: Evaluating 4 years of atmospheric ammonia (NH3) over Europe using IASI satellite observations and LOTOS-EUROS model results, J Geophys Res-Atmos, 119, 9549-9566, 10.1002/2014jd021911, 2014b.

Van Damme, M., Clarisse, L., Dammers, E., Liu, X., Nowak, J. B., Clerbaux, C., Flechard, C. R., Galy-Lacaux, C., Xu, W., Neuman, J. A., Tang, Y. S., Sutton, M. A., Erisman, J. W., and Coheur, P. F.: Towards validation of ammonia (NH3) measurements from the IASI satellite, Atmos Meas Tech, 8, 1575-1591, 10.5194/amt-8-1575-2015, 2015.

Van Damme, M., Whitburn, S., Clarisse, L., Clerbaux, C., Hurtmans, D., and Coheur, P.: Version 2 of the IASI NH3 neural network retrieval algorithm: near-real time and reanalysed datasets Atmos Meas Tech, 239, 10.5194/amt-2017-239, 2017.

Van der Swaluw, E., De Vries, W., Sauter, F., Aben, J., Velders, G., and Van Pul, A.: High-resolution modelling of air pollution and deposition over the Netherlands with plume, grid and hybrid modelling, Atmos Environ, 10.1016/j.atmosenv.2017.02.009, 2017.

van Zanten, M. C., Sauter, F. J., Wichink Kruit, R. J., van Jaarsveld, J. A., and van Pul, M. A. J.: Description of the DEPAC module: Dry deposition modelling with DEPAC_GCN2010, Rivm Report 680180001/2010, RIVM, Bilthoven, Netherlands, 2010.

van Zanten, M. C., Kruit, R. J. W., Hoogerbrugge, R., Van der Swaluw, E., and van Pul, W. A. J.: Trends in ammonia measurements in the Netherlands over the period 1993-2014, Atmos Environ, 148, 352-360, 10.1016/j.atmosenv.2016.11.007, 2017.

Vivanco, M. G., Theobald, M. R., García-Gómez, H., Garrido, J. L., Prank, M., Aas, W., Adani, M., Alyuz, U., Andersson, C., Bellasio, R., Bessagnet, B., Bianconi, R., Bieser, J., Brandt, J., Briganti, G., Cappelletti, A., Curci, G., Christensen, J. H., Colette, A., Couvidat, F., Cuvelier, C., D'Isidoro, M., Flemming, J., Fraser, A., Geels, C., Hansen, K. M., Hogrefe, C., Im, U., Jorba, O., Kitwiroon, N., Manders, A., Mircea, M., Otero, N., Pay, M. T., Pozzoli, L., Solazzo, E., Tsyro, S., Unal, A., Wind, P., and Galmarini, S.: Modeled deposition of nitrogen and sulfur in Europe estimated by 14 air quality model systems: evaluation, effects of changes in emissions and implications for habitat protection, Atmos. Chem. Phys., 18, 10199-10218, 10.5194/acp-18-10199-2018, 2018.

von Bobrutzki, K., Braban, C. F., Famulari, D., Jones, S. K., Blackall, T., Smith, T. E. L., Blom, M., Coe, H., Gallagher, M., Ghalaieny, M., McGillen, M. R., Percival, C. J., Whitehead, J. D., Ellis, R., Murphy, J., Mohacsi, A., Pogany, A., Junninen, H., Rantanen, S., Sutton, M. A., and Nemitz, E.: Field inter-comparison of eleven atmospheric ammonia measurement technique, Atmos. Meas. Tech., 3, 91-112, 2010.

Whitburn, S., Van Damme, M., Clarisse, L., Bauduin, S., Heald, C. L., Hadji-Lazaro, J., Hurtmans, D., Zondlo, M. A., Clerbaux, C., and Coheur, P. F.: A flexible and robust neural network IASI-NH3 retrieval algorithm, J Geophys Res-Atmos, 121, 6581-6599, 10.1002/2016jd024828, 2016.

Whitten, G. Z., Hogo, H., and Killus, J. P.: The Carbon-Bond Mechanism - a Condensed Kinetic Mechanism for Photochemical Smog, Environ Sci Technol, 14, 690-700, DOI 10.1021/es60166a008, 1980.

Wichink Kruit, R. J., van Pul, W. A. J., Otjes, R. P., Hofschreuder, P., Jacobs, A. F. G., and Holtslag, A. A. M.: Ammonia fluxes and derived canopy compensation points over non-fertilized agricultural grassland in The Netherlands using the new gradient ammonia—high accuracy—monitor (GRAHAM), Atmos Environ, 41, 1275-1287, 10.1016/j.atmosenv.2006.09.039, 2007.

Wichink Kruit, R. J., Schaap, M., Sauter, F. J., van Zanten, M. C., and van Pul, W. A. J.: Modeling the distribution of ammonia across Europe including bi-directional surface-atmosphere exchange, Biogeosciences, 9, 5261-5277, 10.5194/bg-9-5261-2012, 2012.

Wichink Kruit, R. J.: ECLAIRE model inter-comparison of atmospheric nitrogen deposition and concentrations over Europe, presentation at the ACCENT-Plus Symposium held in September in Urbino, Italy, 2013.

Zoll, U., Brummer, C., Schrader, F., Ammann, C., Ibrom, A., Flechard, C. R., Nelson, D. D., Zahniser, M., and Kutsch, W. L.: Surface-atmosphere exchange of ammonia over peatland using QCL-based eddy-covariance measurements and inferential modeling, Atmos Chem Phys, 16, 10.5194/acp-16-11283-2016, 2016.